Predictability and Unpredictability in Kalman Filtering

C. I. Byrnes, *Fellow, IEEE*, A. Lindquist, *Fellow, IEEE*, and T. McGregor

Abstract—In this paper, we study the dynamical behavior of the Kalman filter when the given parameters are allowed to vary in a way which does not necessarily correspond to an underlying stochastic system. This may correspond to situations in which the basic parameters are chosen incorrectly through estimates. We show that, as has been suggested by Kalman, the filter equations converge to a limit (corresponding to a steady-state filter) for a subset of the parameter space which is much larger than that corresponding to bona fide stochastic systems. More surprisingly, in the complement of this subset, the filtering equations behave in both a regular and an unpredictable manner, representative of some of the basic aspects of chaotic dynamics. This interesting dynamical behavior occurs already for one-dimensional filters, and we give a complete phase portrait in this case.

I. INTRODUCTION

GIVEN a (scalar) stationary stochastic process $\{y_t; t \in \mathbb{Z}\}$ with an n-dimensional minimal stochastic realization

$$\begin{cases} x_{t+1} = Fx_t + v_t \\ y_t = h'x_t + w_t \end{cases} \quad (1.1)$$

(where $\{v_t, w_t\}$ is white noise and prime denotes transpose), it is well known that the *Kalman filter*

$$\hat{x}_{t+1} = F\hat{x}_t + k_t(y_t - h'\hat{x}_t) \qquad \hat{x}_0 = 0 \quad (1.2)$$

depends only on the covariance data of $\{y_t\}$ and is independent of the particular choice of realization (1.1) [6], [8].

More specifically, the gain sequence $\{k_t\}$ is given by

$$k_t = (1 - h'\Pi_t h)^{-1}(g - F\Pi_t h) \quad (1.3)$$

where $g := E\{x_{t+1}y_t\}$ and $\{\Pi_t\}$ is the solution of the discrete-time matrix Riccati equation

$$\Pi_{t+1} = F\Pi_t F' + (g - F\Pi_t h)(1 - h'\Pi_t h)^{-1}$$
$$\cdot (g - F\Pi_t h)'; \qquad \Pi_0 = 0. \quad (1.4)$$

(This is the invariant Riccati equation of stochastic realization, with $\Pi_t := E\{\hat{x}_t \hat{x}_t'\}$ the covariance of the state estimate.)

Convergence of (1.4), and hence (1.3), is well understood in the classical case when the parameters (F, g, h) correspond to a stochastic system (1.1), but it has been an important open problem to understand precisely for what other parameter values (1.3) will converge to a steady-state value. In the classical case, corresponding, for example, to complete knowledge of the correlation coefficients

$$c_i = E\{y_{t+i}y_t\} \qquad i = 0, 1, 2, \cdots \quad (1.5)$$

of the stationary stochastic process, the parameters (F, g, h) can be determined from the spectral density

$$\Phi(z) = c_0 + \sum_{i=1}^{\infty} c_i(z^i + z^{-i})$$

of $\{y_t\}$. Assuming, as we shall throughout this paper, that $c_0 = E\{y_t^2\} = 1$, these parameters are obtained as a realization of the positive real part

$$\Phi_+(z) = 1/2 + h'(zI - F)^{-1}g \quad (1.6)$$

of $\Phi(z)$. The matrix function Φ_+, being positive real ensures that (F, g, h) corresponds to a stochastic system, or equivalently that the Toeplitz matrices

$$T_t = \begin{bmatrix} c_0 & c_1 & \cdots & c_t \\ c_1 & c_0 & \cdots & c_{t-1} \\ \vdots & \vdots & \ddots & \vdots \\ c_t & c_{t-1} & \cdots & c_0 \end{bmatrix} \quad (1.7)$$

are positive definite for all t. Under these conditions, as $t \to \infty$, the gain sequence $\{k_t\}$ tends to a limit k_∞ and the steady-state Kalman filter is identical to the realization (1.1) with the smallest state covariance P_-. Likewise, $\Pi_t \to P_-$. Moreover, for such classical parameters it is known that the conditions

$$1 - h'\Pi_t h \geq 0 \quad (1.8a)$$

$$1 - h'\Pi_t h = 0 \Rightarrow g - F\Pi_t h = 0 \quad (1.8b)$$

hold for all $t \geq 0$ and, conversely, that if (1.8) holds for all $t \geq 0$, then the parameters correspond to a positive real function (1.6).

However, as pointed out in lectures by Kalman, positivity is not necessary for convergence of the filter, raising the very interesting question of characterizing those values of the parameters (F, g, h) for which (1.3) will converge, leading both to a more complete theoretical understanding of the Kalman filter and to the potential development of "conditioning numbers" for the numerical analysis of filtering prob-

lems. Understanding of the dynamics of (1.3) or (1.4) is also crucial, since one typically will only have estimates of the $\{c_i\}$, and not only questions concerning convergence, but also broader issues such as sensitivity to initial data, become important in applications of the Kalman filter.

This question has also arisen in the study of the fast algorithm

$$\begin{cases} k_{t+1} = \left[1 - \left(h'k_t^*\right)^2\right]^{-1}\left[k_t - \left(h'k_t^*\right)Fk_t^*\right]; & k_0 = g \\ k_{t+1}^* = \left[1 - \left(h'k_t^*\right)^2\right]^{-1}\left[Fk_t^* - \left(h'k_t^*\right)k_t\right]; & k_0^* = g \end{cases}$$

$$(1.9)$$

for Kalman filtering, due to Lindquist [15]. Indeed, some "chaotic" behavior has been observed when this algorithm has been used with parameters (F, g, h) estimated from statistical data. As is suggested by our present results, this is because the sequence (1.5) has lost its positive real property. The fast algorithm (1.9) can be reformulated so that all the parameter dependence enters in the initial conditions and none of the parameters (F, g, h) enters in the recursions themselves [16], thereby reducing the convergence question to one of studying the sensitivity in the initial conditions of a nonlinear dynamical system and to one of determining for which initial conditions there is convergence to a limit point.

For this reason, and because of its intimate connection with spectral factorization, the Kalman filtering algorithm (1.9) allows for a systems theoretic interpretation of the convergence of the Riccati equation (1.4) for nonclassical parameter data, e.g., for initial conditions of the reformulated fast algorithm for which (1.8) holds only for $t \leq T$ but not at time $T + 1$. As we observe (see Remarks 3.11 and 4.6), this situation is a point at which the continuous-time case and the discrete-time case differ in a substantial manner, not in the methods which underlie the analysis of the respective dynamics but rather in the conclusions which we can draw from this analysis. Indeed, our analysis of (1.4) or (1.9) uses a variant of the power method initiated by Vaughan [26], which is the discrete-time analog of Riccati's "state–costate" representation of the Riccati equation (cf. Remark 4.5). It is here, however, that the analogy ends. Consider, for example, a nonclassical choice of parameters as above, where (1.8) is satisfied only in a finite-time interval $[0, T)$. In the continuous-time case, it is well known that for some finite T the trajectory of the Riccati differential equation will escape. This can happen as well for the discrete-time Riccati equation (1.4), e.g., when (1.8b) is violated in the sense that

$$1 - h'\Pi_T h = 0, \qquad g - F\Pi_T h \neq 0$$

However, for nonclassical initial conditions we show that solutions of the fast algorithm can also

1) evolve in unbounded, complicated excursions; or

2) exhibit periodic behavior of every period, $p \geq 3$ (which reduces to $p \geq 2$ for the Riccati equation); or

3) converge to a classical limit.

The situations 1)–2) are of course reminiscent of some of the features of chaotic dynamics. We have, however, refrained from describing these dynamics as being chaotic since

a spectral factorization interpretation implies the existence of certain invariants of motion (see Section III) and therefore these dynamics cannot be topologically or measure-theoretically transitive (as required in some definitions of chaos [7]; see, however, Remark 3.12). On the other hand, 3) is particularly interesting from a systems-theoretic perspective, since convergence to a classical limit occurs when the Riccati equation has lost its variational interpretation, i.e., when (1.8) is violated. Among the results we prove is a general necessary condition for 3) to occur, expressed in terms of spectral factorization. For the one-dimensional case, this is also sufficient, and there is reason to believe that it is true in general (see [5]). As a matter of fact, our preliminary analysis in the higher dimensional case has shown that the Riccati equation admits for more complicated dynamic behavior than the fast algorithms which are lower dimensional, essentially focusing on computing the n-vector $\Pi_t h$ rather than the $n \times n$ symmetric matrix Π_t. This relative simplicity in dimensions $n > 1$ is one reason our basic analysis begins with the fast algorithm, but there are other reasons as well. In particular, using the fast algorithm, one can give a systems-theoretic interpretation of the classical limit of a trajectory with a nonclassical initial condition in terms of spectral factorization and stochastic realizations (see Remarks 3.6 and 4.4).

In order to keep the paper reasonably self-contained and to fix notation, in Section II we present preliminaries on fast filtering algorithms, positive real conditions, and some classical convergence results for Kalman filtering. We begin Section III by stating some results for scalar output systems of arbitrary dimension. In particular, for the fast filtering algorithms, we describe some invariants of motion, a characterization of the equilibrium set and necessary conditions for convergence to a classical limit. For any $p \geq 3$, we claim the existence of initial conditions, of course not satisfying these necessary conditions, which are periodic of period p. Moreover, we also assert the existence of initial data which are arbitrarily close to these periodic points and which have unbounded trajectories, defined for all positive times. Taken together, these results prove that the fast filtering equations are sensitive to initial conditions, in the region of initial data for which there is not convergence to a classical limit.

As we have remarked, convergence is related to a spectral factorization problem; viz. the factorization of a pseudopolynomial canonically associated to the initial data. Based on this pseudopolynomial and its sign definiteness we can give a complete phase portrait for the case of one-dimensional system. In particular, we find that convergence occurs exactly when the pseudopolynomial is sign definite, although not necessarily positive real, on the unit circle. This also turns out to correspond (in the present one-dimensional case) to the condition that the pseudopolynomial has real roots. When this does not occur, the existence of periodic orbits or unbounded excursions depends on whether the phase of such a root is, or is not, a rational multiple of π, yielding what we feel is a surprisingly rich phase portrait in the discrete-time case.

In Section IV, we discuss the ramifications of this phase portrait for the dynamics of the Riccati equation (1.4), which

depends also on the pseudopolynomial introduced in Section III. Of course, each of the corresponding Riccati equations has a measure zero set of initial conditions which escape in finite time. We show that, depending on the phase of the root of this pseudopolynomial, we either have, for initial data which does not escape, convergence, periodic orbits of some period p (all periods $p \geq 2$ are possible), or every orbit being dense. While the first two conclusions are immediate from Vaughan's method, a precise determination of the period and a proof of density require a more refined analysis. Moreover, our interpretation of convergence in the nonclassical case reposes on analysis of the fast filtering algorithm. Section V contains the proofs of our main theorems, providing an analysis of the dynamics via power methods, as well as an explanation of the similarities and differences between the continuous-time and discrete-time cases. In particular, since the continuous-time dynamics either converge or escape in finite time in any dimension, the perhaps plausible expectation that the one-dimensional discrete-time Riccati equation would perhaps behave more like a two-dimensional continuous-time Riccati equation does not explain the presence of both predictable and rather unpredictable dynamical behavior of the discrete-time Kalman filter—a point to which we return in our conclusions, summarized in Section VI.

II. PRELIMINARIES

In this section, we review some relevant facts about the fast algorithms [15]–[17] for Kalman filtering and their relationship to the Szegö polynomials orthogonal on the unit circle [1], [10], [12], the Levinson algorithm [14], positive realness, and classical convergence results.

A version of these algorithms will be our basic tool for analyzing the dynamics of the Kalman filter. The n-dimensional Kalman filter can be characterized by $2n$ parameters and, as we shall see, the fast algorithm can be interpreted as a recursion in the parameter space $\mathbb{R}^{2n}$, generating a sequence of Kalman filters. This naturally brings in questions of positive realness and convergence.

Given a stationary stochastic system (1.1), we have

$$E\{x_{k+1}y_j\} = F^{k-j}g \qquad \text{for } k \geq j \qquad (2.1)$$

where $g := E\{x_1 y_0\}$. From this we obtain the realization

$$c_k = h'F^{k-1}g; \qquad k = 1, 2, \cdots \qquad (2.2)$$

for the covariance sequence $\{1, c_1, c_2, \cdots\}$ of the output process $\{y_0, y_2, y_3, \cdots\}$; for normalization we take $c_0 = 1$. Now, $\{c_k\}$ being a covariance sequence requires that

$$\Phi_+(z) = \frac{1}{2} + h'(zI - F)^{-1}g \qquad (2.3)$$

is positive real, i.e., satisfies the Popov condition

$$\Phi_+(z) + \Phi_+(1/z) > 0 \qquad \text{on the unit circle} \qquad (2.4)$$

and the condition that F is a stability matrix, having all its zeros inside the unit circle.

Another criterion for positive realness of $\Phi_+(z)$ is testing that all Toeplitz matrices $\{T_t, t = 0, 1, 2, \cdots\}$ are positive definite. The study of such Toeplitz forms lead to the Szegö

polynomials $\{\varphi_0(z), \varphi_1(z), \varphi_2(z), \cdots\}$, a sequence of monic polynomial

$$\varphi_t(z) = z^t + \varphi_{t1}z^{t-1} + \cdots + \varphi_{tt} \qquad (2.5)$$

which are orthogonal on the unit circle. The Szegö polynomials are determined from the sequence $\{c_0, c_1, c_2, \cdots\}$ through the polynomial recursions

$$\begin{cases} \varphi_{t+1}(z) = z\varphi_t(z) - \gamma_t \varphi_t^*(z); & \varphi_0(z) = 1 \\ \varphi_{t+1}^*(z) = \varphi_t^*(z) - \gamma_t z\varphi_t(z); & \varphi_0^*(z) = 1 \end{cases} \qquad (2.6)$$

where $\{\gamma_0, \gamma_1, \gamma_2, \cdots\}$ are the Schur parameters

$$\gamma_t = \frac{1}{r_t}\sum_{k=0}^{t}\varphi_{t, t-k}c_{k+1} \qquad (2.7)$$

and $\{r_0, r_1, r_2, \cdots\}$ are given by the recursion

$$r_{t+1} = (1 - \gamma_t^2)r_t; \qquad r_0 = 1. \qquad (2.8)$$

It can be shown that there is a one-to-one correspondence between the subsequences $\{1, c_1, c_2, \cdots, c_t\}$ and $\{\gamma_0, \gamma_1, \ldots, \gamma_{t-1}\}$ for all $t = 1, 2, 3, \cdots$, and that

$$T_t > 0 \Leftrightarrow |\gamma_k| < 1 \qquad \text{for } k = 0, 1, 2, \cdots, t - 1. \qquad (2.9)$$

(See [1], [10], [24].) Consequently, in our analysis the covariance sequence $\{c_t\}$ can be replaced by the sequence $\{\gamma_t\}$ of Schur parameters, and $\Phi_+(z)$ is positive real if and only if all Schur parameters are less than one in modulus, a test that still is infinite but simpler than testing $\{T_t\}$. As we shall see, the fast algorithm serves as a finite dimensional but nonlinear realization of the Schur sequence.

The recursions (2.6)–(2.8) are equivalent to the Levinson algorithm [14]. To see this, note that the two recursions (2.6) are equivalent, $\{\varphi_t^*\}$ being the reversed polynomials

$$\varphi_t^*(z) = \varphi_{tt}z^t + \varphi_{t, t-1}z^{t-1} + \cdots + 1. \qquad (2.10)$$

The connection between Szegö's polynomials and least-squares prediction is well known [12]. In fact, if $\{y_0, y_1, y_2, \cdots\}$ is a stationary purely nondeterministic stochastic process with zero mean and covariance sequence $\{1, c_1, c_2, c_3, \cdots\}$, $c_k := E\{y_t y_{t+k}\}$, then the linear least-squares estimate of y_t given $\{y_0, y_1, \cdots, y_{t-1}\}$ is given by

$$\hat{y}_t = -\varphi_{t1}y_{t-1} - \varphi_{t2}y_{t-2} - \cdots - \varphi_{tt}y_0 \qquad (2.11)$$

where $\{\varphi_{tk}\}$ are the coefficients of the t: th Szegö polynomial. Moreover, the orthogonality of $\{\varphi_t\}$ on the unit circle is equivalent to the orthogonality of the innovation process $\{\tilde{y}_t\}$

$$\tilde{y}_t := y_t - \hat{y}_t = y_t + \varphi_{t1}y_{t-1} + \cdots + \varphi_{tt}y_0 \qquad (2.12)$$

in the inner product $\langle \xi, \eta \rangle = E\{\xi\eta\}$. More specifically, we have

$$E\{\tilde{y}_t\tilde{y}_s\} = r_t\delta_{ts} \qquad (2.13)$$

where $\{r_t\}$ are given by (2.8).

To apply this theory to Kalman filtering, we assume that the stochastic process $\{y_0, y_1, y_2, \cdots\}$ is the output of the stochastic system (1.1) and that, consequently, the covariance

sequence $\{c_1, c_2, c_3, \cdots\}$ is given by the finite-dimensional realization (2.2). The Kalman filter is a recursion updating the linear least-squares estimate $\hat{x}_t$ of x_t given $\{y_0, y_1, \cdots, y_{t-1}\}$. Since $\{\tilde{y}_0, \tilde{y}_1, \cdots, \tilde{y}_{t-1}\}$ is an orthogonal basis of $Y_{t-1} := \text{span}\{y_0, y_1, \cdots, y_{t-1}\}$

$$\hat{x}_t = \sum_{k=0}^{t-1} \frac{1}{r_k} E\{\hat{x}_t \tilde{y}_k\} \tilde{y}_k. \qquad (2.14)$$

However, the components of $(x_t - \hat{x}_t)$ are orthogonal to Y_{t-1}, and therefore (2.14) can be written

$$\hat{x}_t = \sum_{k=0}^{t-1} \frac{1}{r_k} E\{x_t \tilde{y}_k\} \tilde{y}_k. \qquad (2.15)$$

Moreover, $E\{x_{t+1} \tilde{y}_k\} = F E\{x_t \tilde{y}_k\}$ for $k = 0, 1, \cdots, t-1$, and $\tilde{y}_t = y_t - h'\hat{x}_t$, because w_t and v_t are orthogonal to Y_{t-1} which is contained in the past space of the stochastic system (1.1). Therefore (2.15) yields the Kalman filter

$$\hat{x}_{t+1} = F\hat{x}_t + k_t(y_t - h'\hat{x}_t); \qquad \hat{x}_0 = 0 \quad (2.16)$$

where the gain

$$k_t = \frac{1}{r_t} E\{x_{t+1} \tilde{y}_t\} \qquad (2.17)$$

is expressed in a form useful for our purposes. From (2.17) we can derive the Riccati equation (1.3) and (1.4), but here we shall take a different route.

This brings us to the fast algorithms. In view of (2.1), (2.10), and (2.12), the gain (2.17) may be written

$$k_t = \frac{1}{r_t} \varphi_t^*(F) g. \qquad (2.18)$$

This is the key observation that allows us to use the recursions (2.6). In fact, defining

$$k_t^* := \frac{1}{r_t} \varphi_t(F) g \qquad (2.19)$$

it follows from (2.6) and (2.8) that

$$\begin{cases} k_{t+1} = \dfrac{1}{1 - \gamma_t^2}(k_t - \gamma_t F k_t^*); & k_0 = g \\ k_{t+1}^* = \dfrac{1}{1 - \gamma_t^2}(F k_t^* - \gamma_t k_t); & k_0^* = g. \end{cases} \qquad (2.20)$$

It remains to eliminate the Schur parameters $\{\gamma_t\}$. However, inserting (2.2) into the defining relation (2.7), we obtain

$$\gamma_t = h' k_t^* \qquad (2.21)$$

and hence we have a nonlinear realization of the Schur sequence. The system (2.20) with (2.21) inserted in place of γ_t is the fast algorithm (1.9) first presented in [15]. It requires only $2n$ equations to solve for the gain sequence $\{k_t\}$ instead of the $\frac{1}{2}n(n+1)$ equations of the matrix Riccati equation.

Next, following [16], we shall carry this reduction one step further. First, we shall strip the recursions (2.20) of its parameter dependence so that the parameters (F, g, h) occur

only in the initial conditions. To this end, choose the canonical form

$$F = \begin{bmatrix} -a_1 & 1 & 0 & \cdots & 0 \\ -a_2 & 0 & 1 & \cdots & 0 \\ \vdots & \vdots & \vdots & \ddots & \vdots \\ -a_{n-1} & 0 & 0 & \cdots & 1 \\ -a_n & 0 & 0 & \cdots & 0 \end{bmatrix}; \qquad h = \begin{bmatrix} 1 \\ 0 \\ \vdots \\ 0 \end{bmatrix} \quad (2.22)$$

in terms of which we may write

$$F = J - ah' \qquad (2.23)$$

where a is the column vector $(a_1, a_2, \cdots, a_n)'$ and J is the obvious shift matrix. [Consequently, the Kalman filter can be characterized by the $2n$ parameters (a, g)]. Then, observing that $F k_t^* = J k_t^* - \gamma_t a$, the change of variables

$$\begin{cases} q_t := k_t + a \\ q_t^* := k_t^* \end{cases} \qquad (2.24)$$

yields the following "stripped" version of (2.20):

$$\begin{cases} q_{t+1} = \dfrac{1}{1 - \gamma_t^2}(q_t - \gamma_t J q_t^*); & q_o = g + a \\ q_{t+1}^* = \dfrac{1}{1 - \gamma_t^2}(J q_t^* - \gamma_t q_t); & q_o^* = g \end{cases} \qquad (2.25)$$

where $\gamma_t = (q_t^*)_1$, the first component of q_t^*. Therefore, in view of (2.8), the polynomials

$$\begin{cases} Q_t(z) = r_t\left[z^n + (q_t)_1 z^{n-1} + \cdots + (q_t)_n \right] \\ Q_t^*(z) = r_t\left[(q_t^*)_1 z^{n-1} + \cdots + (q_t^*)_n \right] \end{cases} \quad (2.26)$$

satisfy the same recursions

$$\begin{cases} Q_{t+1}(z) = Q_t(z) - \gamma_t z Q_t^*(z) \\ Q_{t+1}^*(z) = z Q_t^*(z) - \gamma_t Q_t(z) \end{cases} \qquad (2.27)$$

as those of the Szegö polynomials (2.6), except that the initial conditions are such that Q_t and Q_t^* have constant degrees n and $n-1$, respectively. From (2.27) it is not hard to see that the functions

$$\frac{1}{r_t}\left[Q_t(z) Q_t(z^{-1}) - Q_t^*(z) Q_t^*(z^{-1}) \right] = D(z, z^{-1})$$

$$(2.28)$$

are invariant for $t = 0, 1, 2, \cdots$. The equations (2.28) provide n first integrals for the system (2.25) and in [16] these integrals are used to obtain an algorithm consisting of only n equations for determining the Kalman gain sequence k_t. Such reduction will play an important role in the following sections.

It is not hard to see (cf. [16]) that $(1/r_t) Q_t(z)$ is the *stable* characteristic polynomial of the matrix $F - k_t h'$ in the Kalman filter

$$\hat{x}_{t+1} = (F - k_t h')\hat{x}_t + k_t y_t \qquad (2.29)$$

and that (q, q^*) tends to a limit $(q_\infty, 0)$ as $t \to \infty$, corresponding to the steady-state Kalman filter. Moreover

$$\Phi_+(z) = \frac{1}{2} + \frac{Q_0^*(z)}{Q_0(z) - Q_0^*(z)}. \qquad (2.30)$$

It readily follows from the invariance (2.28) and the positivity of the parameters $\{r_0, r_1, r_2, r_3, \cdots\}$ that if $\Phi_+(z)$ satisfies the Popov condition (2.4), then so do the rational functions

$$\frac{1}{2} + \frac{Q_t^*(z)}{Q_t(z) - Q_t^*(z)} \qquad (2.31)$$

for all $t = 0, 1, 2, 3, \cdots$. Therefore, since $Q_t(z)$ is stable and the covariance structure of the stochastic system (1.1) is determined by the $2n$ parameters (a, g), each step in the recursion (2.25) defines another stochastic system with $a := q_t - q_t^*$ and $g := q_t^*$.

It should be noted that the subset of the $2n$-dimensional parameter space corresponding to $\Phi_+(z)$ being positive real, i.e., (1.1) being a bona fide (forward) stochastic system, is bounded and simply connected [4]. As an example we may consider the case $n = 1$. Then, setting $z = e^{i\theta}$, the Popov condition (2.3)–(2.4) becomes (after multiplication by $|z + a|^2$)

$$1 + a^2 + 2ag + 2(a + g)\cos\theta > 0 \quad \text{for all } \theta \in [0, 2\pi),$$

i.e.,

$$(1 - |a + g|)^2 > g^2. \qquad (2.32a)$$

Likewise, the stability condition may be written

$$|a| < 1. \qquad (2.32b)$$

Using new coordinates

$$\begin{cases} \alpha = a + g \\ \gamma = g \end{cases} \qquad (2.33)$$

(2.32)–(2.33) defines the positive real diamond-shaped region in Fig. 1.

Moreover, in the case $n = 1$, $\gamma_t = q_t^*$ is the Schur parameter. Therefore, setting $\alpha_t := q_t$, the fast algorithm (2.25) becomes

$$\begin{cases} \alpha_{t+1} = \dfrac{\alpha_t}{1 - \gamma_t^2} \\[2ex] \gamma_{t+1} = -\dfrac{\gamma_t \alpha_t}{1 - \gamma_t^2}. \end{cases} \qquad (2.34)$$

Starting with a bona fide stochastic system, i.e., a pair (α_0, γ_0) inside the diamond, the recursion (2.34) will generate a sequence (α_t, γ_t), each point of which belongs to the diamond and hence corresponds to a stochastic system, converging to $(\alpha_\infty, 0)$, which corresponds to the steady-state Kalman filter

$$\hat{x}_{t+1} = -\alpha_\infty \hat{x}_t + (\alpha_\infty - a) y_t. \qquad (2.35)$$

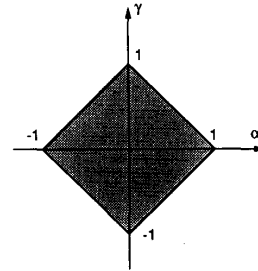The basic question to be addressed in this paper is what

Fig. 1.

happens if the fast filtering algorithm has initial conditions outside the positive real region.

III. MAIN RESULTS CONCERNING THE DYNAMICS OF THE FAST ALGORITHM

To be precise, we need some notations and definitions which we shall, however, give only for open subsets of $\mathbb{R}^N$ rather that the more general case of topological spaces. Let $U \subset \mathbb{R}^N$ be an open subset and consider a continuous map

$$f: U \to U \qquad (3.1)$$

defining a discrete-time dynamical system via

$$x_{t+1} = f(x_t) \qquad x_0 \in U. \qquad (3.1')$$

The forward trajectory

$$\Theta(x_0) = \{x_t; t = 1, 2, 3, \cdots\}$$

is called the *orbit* of x_0. Thus $\Theta(x_0)$ is finite if and only if x_0 lies on a periodic orbit in which case we say that x_0 is a *periodic point of period n*, where n is the smallest nonnegative integer such that $f^n(x_0) = x_0$. The dynamical system $(3.1)'$ is said to be *sensitive to initial data* provided that for any $x_0 \in U$, and, for all $\delta > 0$ and all neighborhoods V of x_0 there exists $x_0' \in V$ and n such that

$$\|f^n(x_0') - f^n(x_0)\| > \delta. \qquad (3.2)$$

Remark 3.1: The existence of periodic points of arbitrarily high period and sensitivity to initial data are two of the principal manifestations of chaotic dynamics. Many authors (see, e.g., [7]) also require some kind of transitivity or irreducibility, in either a topological or a measure-theoretic sense. For example, the dynamical system $(3.1')$ is said to be *topologically transitive* if for any two open subsets $V_1, V_2 \subset U$ there exists an $n \geq 0$ such that $f^n(V_1) \cap V_2 \neq \emptyset$. Thus, if $(3.1')$ has a dense orbit, then $(3.1')$ is topologically transitive. As it turns out, the fast algorithms for Kalman filtering, as well as the discrete-time Riccati equation, do exhibit periodic behavior of every period p, $p \geq 3$ or $p \geq 2$, respectively, and sensitivity to initial conditions. As we shall see, the dynamical system (2.25) is not, however, topologically transitive, and for this reason, we have refrained from claiming that the filtering algorithm exhibits chaos, although there is still no uniform agreement on what actually constitutes chaotic dynamics.

The fast algorithms for Kalman filtering fail to be topologi-

cally transitive because they possess symmetries and have conserved quantities, i.e., integrals of motion. For example, the dynamical system (2.25) is invariant under the transformation

$$(q, q^*) \rightarrow (q, -q^*). \qquad (3.3)$$

Moreover, comparing coefficients of $(z^i + z^{-i})$ in (2.28) we obtain $n + 1$ equations in $2n$ variables, which after dividing by the equation corresponding to $i = 0$ yields n invariant rational quantities

$$h_i(q, q^*) = \text{constant}. \qquad (3.4)$$

Theorem 3.2: The common level sets of the functions $h_i(q, q^*)$, $i = 1, 2, \cdots, n$, are invariant under the dynamical system (2.25); (2.25) is also invariant under the transformation (3.3). In particular, the dynamical system (2.25) is not topologically transitive.

Proof: Consider the vector function $h: \mathbb{R}^n \rightarrow \mathbb{R}^n$ with h_i, $i = 1, 2, \cdots, n$, as components. Choose any two open subsets U_1, V_1 intersecting *image*(h) disjointly. Then, $U = h^{-1}(U_1)$, $V = h^{-1}(V_1)$ are two disjoint open subsets of $\mathbb{R}^{2n}$, so that $f^t(U) \cap V = \varnothing$ for all $t \in \mathbb{N}$. $\qquad \square$

The invariants (3.4) can also be interpreted in terms of spectral factorization. In fact, defining the polynomials

$$\begin{cases} a_t(z) = \dfrac{1}{r_t}[Q_t(z) - Q_t^*(z)] \\[2mm] b_t(z) = \dfrac{1}{r_t}[Q_t(z) + Q_t^*(z)] \end{cases} \qquad (3.5)$$

(2.28) may be written

$$r_t[a_t(z)b_t(z^{-1}) + a_t(z^{-1})b_t(z)] = 2D(z, z^{-1}) \quad (3.6)$$

or equivalently

$$\frac{b_t(z)}{2a_t(z)} + \frac{b_t(z^{-1})}{2a_t(z^{-1})} = \frac{d_t(z, z^{-1})}{a_t(z)a_t(z^{-1})} \qquad (3.7)$$

where $d_t(z, z^{-1}) = r_t^{-1}D(z, z^{-1})$. Now, if the pseudopolynomial $D(z, z^{-1})$ is *sign definite*, i.e., $D(z, z^{-1})$ is either nonnegative or nonpositive for all z on the unit circle, then so is

$$d_t(z, z^{-1}) = a_t(z)b_t(z^{-1}) + a_t(z^{-1})b_t(z) \quad (3.8)$$

for all t along the trajectory of the dynamical system (2.25). Then, modulo sign, (3.7) is a spectral density. In particular, the rational function

$$\Phi_+(z) = \frac{b_t(z)}{2a_t(z)} \qquad (3.9)$$

is *positive real* if and only if d_t is positive, and $a_t(z)$ is stable, i.e., a Schur polynomial. Then, of course, $b_t(z)$ is also stable [6], [8].

Theorem 3.3:

1) The equilibrium set of the dynamical system (2.25) consists of all points having the form $(q_\infty, 0)$. A necessary condition for convergence of (q_t, q_t^*) to an equilibrium is

sign definiteness of the pseudopolynomial $D(z, z^{-1})$ defined in (3.28) and computed, for example, from (q_0, q_0^*). In this case, $Q_\infty(z)$ is a spectral factor of $r_\infty D(z, z^{-1})$.

2) The domain of attraction of the stable equilibria $(q_\infty, 0)$ contains the "positive real systems," i.e., those initial data (q_0, q_0^*) for which $D(z, z^{-1})$ is positive and the polynomial $a_0(z)$ is a Schur polynomial. In this case, $Q_t(z)$ is a Schur polynomial for all $t = 0, 1, 2, \cdots$, and $Q_\infty(z)$ is a stable spectral factor of $r_\infty D(z, z^{-1})$.

3) The sign indefinite region consisting of those (q_0, q_0^*) for which $D(z, z^{-1})$ is not sign definite contains invariant submanifolds on which there are infinitely many periodic points of any period p, $p \geq 3$, and on which the restricted dynamics is sensitive to initial data.

Remark 3.5: This theorem, which we shall prove in Section V, gives a partial answer, in the case studied above, to the question posed in [11]. The natural conjecture extending 2), that the dimension of the stable manifold of an equilibrium $(q_\infty, 0)$ is equal to the number (counted with multiplicity) of roots of $Q_\infty(z)$ inside the unit disk, has just been proven in [5]. Finally, simulations indicate that the invariant submanifold referred to in 3) is in fact an invariant open subset, and we expect to have more to say about this for $n > 1$ in a future paper. A procedure for spectral factorization based on principles akin to those in [15], [16], and hence to those used here, can be found in [9]. $\qquad \square$

We now illustrate the use of the integral invariants derived in Theorem 3.2 by giving a complete description of the phase portrait of (3.25) in the case $n = 1$. Then, as already pointed out in Section II, $q_t^* = \gamma_t$ and, with $a_t := q_t$ (3.25) takes the form

$$\begin{cases} \alpha_{t+1} = \dfrac{\alpha_t}{1 - \gamma_t^2} \\[3mm] \gamma_{t+1} = \dfrac{-\gamma_t\alpha_t}{1 - \gamma_t^2}. \end{cases} \qquad (3.10)$$

Moreover, (2.28) becomes

$$r_t[(z + \alpha_t)(z^{-1} + \alpha_t) - \gamma_t^2] = D(z, z^{-1}) \quad (3.11)$$

from which the sign definite region can be determined. In fact

$$D(e^{i\theta}, e^{-i\theta}) = 1 + \alpha_0^2 - \gamma_0^2 + 2\alpha_0 \cos\theta \quad (3.12)$$

which is nonnegative in regions I, III, and IV in Fig. 2, nonpositive in region II, and sign indefinite in the "white corridors" which we shall refer to as the *sign indefinite corridors*. Each of the sign definite regions has been divided into two, one marked in Fig. 2 with index +, the other with −. We shall see that Theorem 3.2 implies that an orbit which starts in a plus (minus) region must remain in the union of plus (minus) regions.

If $\alpha_0 \neq 0$, the invariant (3.11) yields two equations which after elimination of r_t yield

$$1 + \alpha_t^2 - \gamma_t^2 = \frac{2}{\kappa}\alpha_t \qquad (3.13)$$

where κ is a constant. According to Theorem 3.2, an initial
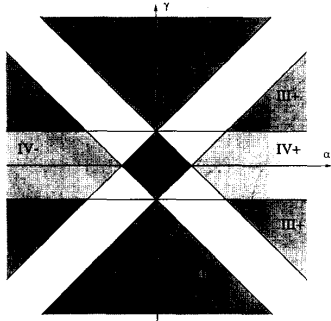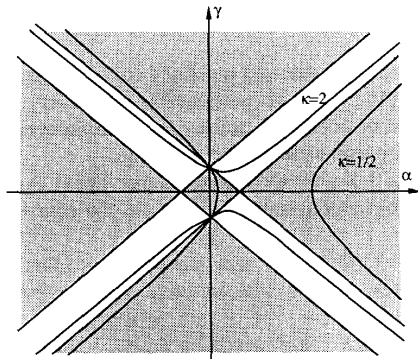
Fig. 2.

Fig. 3.

condition (α_0, γ_0) lying on the hyperbola (3.13) gives rise to an orbit lying on (3.13). Fig. 3 depicts these hyperbolas for $\kappa = 1/2$ and $\kappa = 2$. In general, hyperbolas for which $\kappa^2 < 1$ lie in the sign definite regions, those for which $\kappa^2 > 1$ lie in the sign indefinite corridors, and when $\kappa^2 = 1$, they degenerate to form the boundary between the sign definite and sign indefinite regions. Theorem 3.2 also states that the system (3.10) is invariant under the transformation $(\alpha, \gamma) \rightarrow (\alpha, -\gamma)$. If $\alpha_0 = 0$ and $|\gamma_0| \neq 1$, corresponding to the case $\kappa = 0$, (3.10) converges to $(0, 0)$ in just one iteration. This corresponds to the occurrence of invariant directions in the related Riccati equation, as explained in [16] and further developed in [23]. If $|\gamma_0| = 1$, there is finite escape.

Theorem 3.2,1) asserts that sign definiteness is a necessary condition for convergence. In Section V, we shall show that it is sufficient. Among the results we prove are the following.

Theorem 3.5:

a) Suppose $0 < \kappa^2 < 1$. The hyperbola (3.13) contains two equilibria $(\alpha_\pm, 0)$, where $\alpha_\pm = (1 \mp \sqrt{1 - \kappa^2})/\kappa$. Here $(\alpha_+, 0)$ is a stable equilibrium, $(\alpha_-, 0)$ is an unstable equilibrium and all other initial data (α_0, γ_0) on this hyperbola give rise to an orbit which either converge to $(\alpha_+, 0)$ or escape to infinity after finitely many iterations.

1) In the first case, initial data lying in regions $IV_+(IV_-)$ give rise to trajectories for which $|\alpha_t|$ increases monotonically until $(\alpha_{t+1}, \gamma_{t+1})$ jumps to region III_+ (III_-). For any

point (α_0, γ_0) in region III_+ (III_-), (α_1, γ_1) jumps to region II_+ (II_-), and in turn, any point (α_0, γ_0) in region II_+ (II_-) jumps to I_+ (I_-) with $|\alpha_1| > |\alpha_0|$. For any initial condition (α_0, γ_0) in region I_+ (I_-), (α_t, γ_t) converges to $(\alpha_+, 0)$ with $|\alpha_t|$ monotonically increasing to $|\alpha_+|$.

2) (α_t, γ_t) escapes after finitely many iterations only if (α_0, γ_0) lies in regions IV_+ or IV_-. There is a unique pair of points $(\alpha_0^{(i)}, \pm \gamma_0^{(i)})$ which escape after i iterations [given explicitly in (5.13)] and the sequences $(\alpha_0^{(i)}, \pm \gamma_0^{(i)})$ converge, monotone decreasing in $|\alpha_0^{(i)}|$ to $(\alpha_-, 0)$.

b) When $\kappa^2 = 1$, the invariant manifold (3.13) degenerates to the two boundary lines, passing through $(\kappa, 0)$, between the sign definite and sign indefinite regions. There is one equilibrium $(\alpha_+, 0) := (\kappa, 0)$ and it is stable. Other initial conditions (α_0, γ_0) give rise to an orbit which either converges to $(\alpha_+, 0)$ in the manner described in point 1) above, or escapes in finite time. In the latter case the statement of point 2) holds except that $\alpha_- = \alpha_+$.

Remark 3.6: As we have just seen, each point (α_0, γ_0) in the diamond of Fig. 1 corresponds to a positive real function

$$v(z) = \frac{1}{2} \frac{z + b}{z + a}$$

with $a = \alpha_0 - \gamma_0$ and $b = \alpha_0 + \gamma_0$, and vice versa. We have shown that each such point with $\alpha_0 \neq 0$ lies on a hyperbola containing two equilibria, $(\alpha_+, 0)$ and $(\alpha_-, 0)$ for the dynamical system (3.10). With initial condition (α_0, γ_0), (α_t, γ_t) tends to $(\alpha_+, 0)$ in forward time (Theorem 3.5) and to $(\alpha_-, 0)$ in backward time (Section V). Since, $r_t = \alpha_0/\alpha_t$, an immediate consequence of (3.10) and (2.8), it follows therefore from (3.11) that

$$D(z, z^{-1}) = \frac{\alpha_0}{\alpha_+}(z + \alpha_+)(z^{-1} + \alpha_+)$$

$$= \frac{\alpha_0}{\alpha_-}(z + \alpha_-)(z^{-1} + \alpha_-)$$

and consequently (3.7) implies that

$$v(z) + v(1/z) = \frac{\alpha_0}{\alpha_+} \frac{(z + \alpha_+)(z^{-1} + \alpha_+)}{(z + a)(z^{-1} + a)} \quad (3.14a)$$

$$= \frac{\alpha_0}{\alpha_-} \frac{(z + \alpha_-)(z^{-1} + \alpha_-)}{(z + a)(z^{-1} + a)} \quad (3.14b)$$

yielding the two stable minimal spectral factors, W_+ and W_-, respectively, of the spectral density (3.14). When $\alpha_0 = 0$, (α_t, γ_t) tends in one step (in forward time) to $(0, 0)$ but escapes in backward time, so that only one spectral factor is produced. This is in agreement with the fact that $D(z, z^{-1}) = 1 - \gamma_0^2$ is degree zero in this case.

What is then the systems-theoretic meaning of the convergence from points in the other shaded regions in Fig. 2 or Fig. 3? The points (α_0, γ_0) in regions III and IV [region II] correspond precisely to the functions for which $v(1/z)$ is positive real [negative real]. In fact, the positive real function $\hat{v}(z) := v(1/z)$ is represented by the point $(\hat{\alpha}, \hat{\gamma})$ in the diamond where $\hat{\alpha} := \alpha/ab$ and $\hat{\gamma} := \gamma/ab$, located on the

same hyperbola. (Note that $ab = \alpha_0^2 - \gamma_0^2 \geq 1$). Again $v(z)$ satisfies (3.14), but now the spectral factors, $\overline{W}_+$ and $\overline{W}_-$, are antistable, corresponding to backward stochastic realizations [18], [19]. In particular, $\overline{W}_+$ is the transfer function of a backward steady-state Kalman filter, just as W_+ is that of a forward one. The negative regions II are just transitional for the dynamical system, being visited only once when α_t jumps over infinity.   □

In Section V, we give explicit expressions for the points which escape in finite time, both for the cases of Theorem 3.5 and when $1 < \kappa^2 \leq \infty$. In continuous-time filtering (cf. Remark 3.11 and Section V) it is of course the case that whenever the "positive real" condition is violated, finite escape time occurs. We recall from Section II that the Popov criterion implies that only initial data in the diamond-shaped region I_-, I_+ correspond to positive real systems, yet Theorem 3.5 implies that the initial data in the shaded region which do not escape in finite time have trajectories which actually converge. This is in sharp contrast to the continuous-time case, a contrast which persists for the Riccati equation (see Section IV). Moreover, while convergence is unexpectedly admirable, nonpathological behavior in a nonclassical setting, the "the white corridors" of Fig. 2 support much more exotic dynamic behavior.

Theorem 3.7: Let κ be such that $1 < \kappa^2 \leq \infty$. Then one of two alternatives hold:

1) arctan $\sqrt{\kappa^2 - 1} \in \mathbb{Q}\pi$ in which case every initial condition on (3.13) either escapes in finite time or is a periodic point of period p, where

$$\frac{1}{2} \arctan \sqrt{\kappa^2 - 1} = \frac{q}{p}\pi, \qquad (q, p) = 1$$

if $\kappa < -1$ and

$$\frac{1}{2}\left\{\pi - \arctan \sqrt{\kappa^2 - 1}\right\} = \frac{q}{p}\pi, \qquad (q, p) = 1$$

if $\kappa > 1$. Moreover, if p is odd, there are precisely $2(p - 1)$ points which escape, and these escape two each at times $1, \cdots, p - 1$, and, if p is even, there are $(p - 2)$ points escaping two each at times $1, 2, \cdots, p/2 - 1$. (This includes the case $\kappa^2 = \infty$ when all points have period four excepting two initial conditions which escape in one step.)

2) arctan $\sqrt{\kappa^2 - 1}$ and π are rationally independent, in which case any initial condition on (3.13) has a dense orbit or escapes in finite time. The set of points which escape is a countable dense subset of the hyperbola, having a dense complement.

There are several interesting corollaries to Theorem 3.5 and 3.7. The first asserts that in the sign indefinite corridor, the dynamics (3.10) can be highly regular.

Corollary 3.8: In the sign indefinite corridors the dynamical system (3.10) has a dense set of periodic points. Moreover (3.10) has infinitely many periodic points of any period p, $p \geq 3$. More explicitly, for arctan $\sqrt{\kappa^2 - 1} \in \mathbb{Q}\pi$ there are two cases. If $\kappa < -1$, then periodic orbits exist of every period $p \geq 4$. For $\kappa > 1$, periodic orbits exist of every period $p \geq 3$, except $p = 6$.
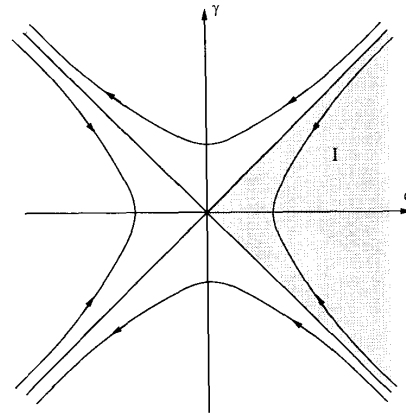

Fig. 4.

Corollary 3.9: In the sign indefinite corridors the dynamical system (3.10) has an uncountable dense set of points which escape in finite time and an uncountable dense set of points which generate an unbounded orbit.

Corollaries 3.8 and 3.9 taken together assert that (3.10) exhibits highly unpredictable behavior in the sign indefinite corridors.

Corollary 3.10: In the sign indefinite corridors the dynamical system (3.10) exhibits sensitive dependence on initial data.

Proof: For any initial condition $(\alpha_0\gamma_0)$, either (α_0, γ_0) escapes in finite time, generates a dense set of first coordinates α_t, or is periodic. In the first two cases, any neighborhood V of (α_0, γ_0) contains a periodic point (α_0', γ_0') so that for all δ there exists an n such that

$$\|f^n(\alpha_0, \gamma_0) - f^n(\alpha_0', \gamma_0')\| > \delta.$$

If the third alternative holds, then in any neighborhood V of (α_0, γ_0) there is a (α_0', γ_0') generating dense set of first coordinates α_t', so that for all $\delta > 0$ there exists an n such that the inequality above holds.   □

Remark 3.11: In continuous time the fast algorithms for Kalman filtering in one dimension take the form

$$\begin{cases} \dot{\alpha} = -\gamma^2 \\ \dot{\gamma} = -\gamma\alpha \end{cases} \qquad (3.15)$$

which admits the integral invariant $H(\alpha, \gamma) = \alpha^2 - \gamma^2$. Fig. 4 depicts the integral curves of this system and the set I of initial data corresponding to a positive real system. It is an elementary (and well known) calculation that finite escape time occurs for any initial data lying outside of region I, in sharp contrast to the phase portrait in discrete time described by Theorems 3.5–3.7. In the next section, we illustrate these distinctions in terms of Kalman filtering and Riccati equations.   □

Remark 3.12: Our analysis of the fast filtering algorithm evolving on the hyperbola (3.13) is essentially equivalent to an analysis of a parameterized nonlinear system

$$\alpha_{t+1} = f(\kappa, \alpha_t) \qquad (3.16)$$

in one dimension. The somewhat exotic variation of the behavior of (3.16) with the parameter κ is perhaps reminiscent of the chaos exhibited by the dynamical system

$$\alpha_{t+1} = \kappa \alpha_t - \kappa \alpha_t^2, \qquad 0 \le \kappa \le 4 \qquad (3.17)$$

modeled by a quadratic map on the interval $[0, 1]$ into itself, especially after period doubling has subsided, i.e., for $\kappa > 3.45 \cdots$, and before the onset of chaos. In this range, there are stable periodic points of arbitrarily high-order periods, and for certain parameter values there also exist dynamics with dense orbits as well as dynamics having a Cantor-like set as an attractor. The differences between the dynamical behavior of the parameter dependent systems (3.16) and (3.17) are reflected in two features. First, for those values of κ for which (3.16) has periodic points, a finite number of points escape in finite time, and the rest are all periodic. Arbitrarily close to such a κ there exists κ' such that for (3.16) every orbit is dense (or escape in finite time). In contrast, there are values of κ for which (3.17) has periodic orbits, which are stable and so persist under small perturbations of κ. In this sense (3.16) is always more sensitive to initial data. On the other hand, only two possibilities exist for (3.16), viz. either critically stable periodic points or all orbits dense, and it is not possible to have a more elaborate attractor. However, for $\kappa = 4$ the system (3.17) is known [7] to exhibit all three kinds of behavior simultaneously, thereby being chaotic in the sense of [7] (see also Remark 3.1).

IV. A DISCUSSION OF CONSEQUENCES FOR DISCRETE-TIME RICCATI EQUATIONS AND KALMAN FILTERING

Periodic, quasiperiodic, as well as more classical convergent behavior for the "power method" models of quite general discrete-time Riccati equations, and consequently, for such Riccati equations themselves, has been known at an abstract geometric level for some time (see [2], [22]). One of the new consequences of our analysis of the fast algorithms for Kalman filtering is that on the one hand some fairly exotic behavior exists not only for general mathematical anomalies but even for Riccati equations arising in Kalman filtering. As we shall see, whereas in continuous time it is well known that Riccati equations always have finite escape time in the absence of the appropriate positive real conditions, this is not the case in discrete time. Moreover, not only will there exist (for arbitrary dimensions) both periodic behavior and sensitivity to initial data when the positive real conditions are violated, but convergence to a classical limit may also occur. The system-theoretic interpretation of this unanticipated event, which does not have a continuous-time analog, is provided by an analysis of the corresponding fast filtering algorithms. In fact, writing the Riccati equation (1.4) in the form

$$\Pi_{t+1} - \Pi_t = \Lambda(\Pi_t) \qquad (4.1)$$

where $\Lambda: \mathbb{R}^{n \times n} \to \mathbb{R}^{n \times n}$ is defined as

$$\Lambda(P) = FPF' - P$$
$$+ (g - FPh)(1 - h'Ph)^{-1}(g - FPh)' \qquad (4.2)$$

the structure of the fast filtering algorithms is reflected in the fact that the initial condition $\Pi_0 = 0$ renders $\Lambda(\Pi_0) = gg'$ nonnegative definite and low rank, a property which, as explained in Section II, is preserved along the trajectory so that

$$\Lambda(\Pi_t) = r_t q_t^* q_t^{*\prime} \qquad (4.3)$$

(cf. [15], [16]). Therefore, to study the fast algorithms for Kalman filtering is to study a particular part of the phase portrait of the Riccati equation. Nevertheless, as we shall see in this paper for the case $n = 1$, the phase portraits of the fast algorithms provide a conceptual framework for understanding the complete picture, not only the part related to filtering. Here, we will confine our discussion to the one-dimensional case, where a good deal of interesting phenomena already occurs and where we have a complete phase portrait.

Consider the one-dimensional stochastic system

$$\begin{cases} x_{t+1} = -ax_t + v_t \\ y_t = x_t + w_t \end{cases} \qquad (4.4)$$

where $\{v_t, w_t\}$ is white noise, and the system is in steady state so that $\{x_t, y_t\}$ are jointly stationary processes. As before, we assume that $E\{y_t^2\} = 1$. Then the linear least squares estimate $\hat{x}_t$ of x_t given the observations $\{y_0, y_1, \cdots y_{t-1}\}$ is determined, for $t = 0, 1, 2, \cdots$, by the Kalman filter

$$\hat{x}_{t+1} = -a\hat{x}_t + k_t(y_t - \hat{x}_t); \qquad \hat{x}_0 = 0. \qquad (4.5)$$

Here, the *gain sequence* $\{k_t\}$ is given by

$$k_t = \frac{\gamma_0 + a\pi_t}{1 - \pi_t} \qquad (4.6)$$

where $\gamma_0 := E\{y_1 y_0\}$ and $\{\pi_t\}$ is the solution of the discrete Riccati equation

$$\pi_{t+1} = a^2 \pi_t + \frac{(\gamma_0 + a\pi_t)^2}{1 - \pi_t}; \qquad \pi_0 = 0. \qquad (4.7)$$

Clearly, the Kalman filter depends only on the two parameters (a, γ_0), but if they are to come from a stochastic system, only certain pairs (a, γ_0) are allowed, namely, precisely those for which the point (α_0, γ_0), with

$$\alpha_0 := a + \gamma_0 \qquad (4.8)$$

belongs to the open diamond-shaped region in Fig. 1 derived from the Popov criterion. It follows from well-known results in Kalman filtering theory that, for (α_0, γ_0) in this region, the solution of the Riccati equation converges to a limit π_∞ which is identical to p_+, the minimum solution of the algebraic Riccati equation $\Lambda(p) = 0$.

In terms of the fast filtering algorithm (3.10), the solution of the Riccati equation (4.7) is

$$\pi_t = \frac{\alpha_t - \alpha_0}{\alpha_t} \qquad (4.9)$$

and the Kalman filter

$$\hat{x}_{t+1} = -\alpha_t \hat{x}_t + (\alpha_t - \alpha_0 + \gamma_0)y_t \qquad (4.10)$$

can be readily computed from (3.10). The Kalman filter can clearly be defined for any pair (α_0, γ_0), and understanding the dynamic behavior of the filtering algorithms for (α_0, γ_0) not generated by an underlying stochastic system is important for understanding problems created by inaccurate parameter estimates.

It follows from Theorem 3.5 that the convergent region of the (α_0, γ_0)-plane is much larger than the subset (depicted in Fig. 1) for which the stochastic system interpretation holds. In fact, the subset $\{(\alpha_0, \gamma_0): |\kappa| < 1\}$ is the shaded region in Fig. 2 and consequently (excluding a subset of the (α, γ)-plane of measure zero for which there is finite escape time) the Kalman filter makes sense as long as its initial conditions lie in the shaded region, and it will converge to a steady-state Kalman filter which has a proper stochastic interpretation. In fact, in finite time, in a manner described in Theorem 3.5, (α_t, γ_t) will lie in diamond of Fig. 1 and will stay there. Hence, even if the original, "misaligned" parameters did not correspond to a stochastic system, in a finite number of steps the system will remarkably evolve to a system which has such an interpretation provided the initial data lies in the shaded region. However, if (α_0, γ_0) lies in the white corridors of Fig. 2, the Kalman filter will behave erratically and there will be no convergence to a steady-state Kalman filter.

These interesting properties of the fast filtering algorithm carries over to the Riccati equation (4.7) via (4.9). This is immediate if $\pi_0 = 0$ (as in Kalman filtering), but the following theorem is stated for an arbitrary initial condition π_0. First, however, we note that the Riccati equation (4.7) may be written

$$\pi_{t+1} - \pi_t = \frac{\varphi(\pi_t)}{1 - \pi_t} \qquad (4.11)$$

where φ is the polynomial

$$\varphi(p) = p^2 - 2\left(1 - \frac{\alpha_0}{\kappa}\right)p + \gamma_0^2 \qquad (4.12)$$

and κ is the constant

$$\kappa = \frac{2\alpha_0}{1 + \alpha_0^2 - \gamma_0^2} \qquad (4.13)$$

appearing in the integral relation (3.13).

Theorem 4.1: Consider the Riccati equation corresponding to (α_0, γ_0), and let κ be defined by (4.13). Then, there is finite escape only if $\varphi(\pi_0) \geq 0$, and then only for π_0 in a subset of the real line of measure zero. For all other π_0

1) $\{\pi_t\}$ converges if and only if $|\kappa| \leq 1$. The zeros p_+, p_- of φ are equilibrium points, and $\pi_t \to p_+ \leq p_-$ except when $\pi_0 = p_-$.

2) $\{\pi_t\}$ is periodic if and only if $1 < |\kappa| \leq \infty$ and

$$\arctan \sqrt{\kappa^2 - 1} = \frac{n}{d}\pi$$

for some $n, d \in \mathbb{Z}$ (Here we take $\arctan(\infty) = \pi/2$). If n and d are coprime, the period is d.

3) $\{\pi_t\}$ is dense on the real line if and only if $|\kappa| > 1$

and

$$\arctan \sqrt{\kappa^2 - 1} \notin \mathbb{Q}\pi.$$

Moreover, for each fixed π_0, the subset of points (α_0, γ_0) for which there is finite escape is of measure zero. Also, for each $d = 2, 3, 4, \cdots$ there are infinitely many parameter pairs (α_0, γ_0) such that all trajectories of the Riccati equation are periodic of period d.

Corollary 4.2: If, in the dynamical system (3.10), (α_0, γ_0) is periodic with period p then the trajectories of the corresponding Riccati equation have period p if p is odd and period $p/2$ if p is even.

Corollary 4.3: If $\varphi(\pi_0) \geq 0$, the orbit $\{(\alpha_t, \gamma_t)\}$ of $(\bar{\alpha}_0, \bar{\gamma}_0)$, where $\bar{\alpha}_0 := \alpha_0/(1 - \pi_0)$ and $\bar{\gamma}_0 := \sqrt{|\varphi(\pi_0)|}/(1 - \pi_0)$, under the dynamical system

$$\begin{cases} \alpha_{t+1} = \dfrac{\alpha_t}{1 - \gamma_t^2} \\[2mm] \gamma_{t+1} = \dfrac{-\alpha_t\gamma_t}{1 - \gamma_t^2} \end{cases} \qquad (4.14)$$

belongs to the integral curve (3.13), i.e.,

$$1 + \alpha_t^2 - \gamma_t^2 = 2\alpha_t/\kappa \qquad (4.15)$$

and $\{\pi_t\}$ is given by

$$\pi_t = 1 - \alpha_0/\alpha_t. \qquad (4.16)$$

If $\varphi(\pi_0) \leq 0$, the orbit $\{(\bar{\alpha}_t, \bar{\gamma}_t)\}$ of $(\bar{\alpha}_0, \bar{\gamma}_0)$ under the dynamical system

$$\begin{cases} \alpha_{t+1} = \dfrac{\alpha_t}{1 + \gamma_t^2} \\[2mm] \gamma_{t+1} = \dfrac{-\alpha_t\gamma_t}{1 + \gamma_t^2} \end{cases} \qquad (4.17)$$

belongs to the integral curve

$$1 + \alpha_t^2 + \gamma_t^2 = 2\alpha_t/\kappa \qquad (4.18)$$

and $\{\pi_t\}$ is given by (4.16). The second case only occurs if $|\kappa| \leq 1$.

This corollary can be understood from the fact that if $\varphi(\pi_0) \geq 0$ then $\varphi(\pi_t) \geq 0$ for all positive t so that (4.11) may be written

$$\pi_{t+1} - \pi_t = r_t\gamma_t^2 \qquad (4.19)$$

where $r_t := 1 - \pi_t$, for some sequence $\{\gamma_t\}$ which turns out to be identical to the one in the corollary. We can retain these formulas in the case when $\varphi(\pi_0) \leq 0$ by merely exchanging $\{\gamma_t\}$ formally by the sequence $\{i\gamma_t\}$ on the imaginary axis. The integral curves of the Corollary 4.2 are illustrated in Fig. 5 for $|\kappa| < 1$. In this case, there are two sets of curves, corresponding to (4.15) and (4.18), respectively, whereas when $|\kappa| > 1$ only the white corridor hyperbolas occur.

Remark 4.4: The dynamical system (4.17) has an important interpretation in *stochastic realization theory*, specifically, in terms of the procedure described in [18, p. 383]. In fact, the class of stochastic systems (4.4) having a fixed prescribed pair (α_0, γ_0) of parameters in the diamond of Fig.
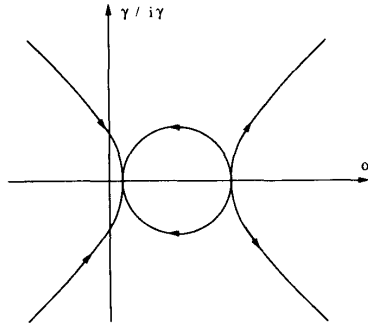
Fig. 5.

1, and hence the same Kalman filter, can be parameterized by their covariances $\pi_0 := E\{x_0 x_0'\}$: they are precisely all π_0 on the closed interval $[p_+, p_-]$. There is a two-dimensional normalized white noise $\{u_t, \text{ with } (E\{u_t u_s'\} = I\delta_{ts})$ such that

$$\begin{bmatrix} w_t \\ v_t \end{bmatrix} = \begin{bmatrix} b \\ d \end{bmatrix} u_t \quad \text{where} \quad \begin{bmatrix} b \\ d \end{bmatrix} = \begin{bmatrix} b_1 & b_2 \\ r_0^{1/2} & 0 \end{bmatrix} \quad (4.20)$$

and where $r_0 := 1 - \pi_0$. Now, defining $(\bar{\alpha}_0, \bar{\gamma}_0)$ by

$$\begin{cases} \bar{\alpha}_0 = (1 - \pi_0)^{-1/2} b_1 + a \\ \bar{\gamma}_0 = (1 - \pi_0)^{-1/2} b_2 \end{cases} \quad (4.21)$$

the realization with covariance π_k has white noise intensity

$$\begin{bmatrix} b \\ d \end{bmatrix}_k = \sqrt{\frac{\alpha_0}{\bar{\alpha}_k}} \begin{bmatrix} \bar{\alpha}_k - a & \bar{\gamma}_k \\ 1 & 0 \end{bmatrix} \quad (4.22)$$

where we have used index k to remind ourselves that this is not time. In particular $b_2 = 0$ corresponds precisely to the equilibrium points p_+ and p_-. □

Remark 4.5: Since the Riccati equation (4.7) can be expressed in terms of iterating a simple Möbius transformation

$$\pi_{t+1} = \frac{(\alpha_0^2 - \gamma_0^2)\pi_t + \gamma_0^2}{1 - \pi_t} \quad (4.7')$$

there are of course some very direct methods for verifying Theorem 4.1, which are especially simple in the one-dimensional case. By the fundamental theorem of projective geometry (see e.g., [3]) any Möbius transformation has a realization in two dimensions as a linear transformation acting on lines through 0, very much the same as Riccati's derivation of the Riccati differential equation. In discrete-time filtering and control, this state–costate representation of the Riccati differential equation was discovered by Vaughan [26] and we want to thank one of the referees for deriving Theorem 4.1, 1) and 2) via Vaughan's method, which is also known in numerical analysis as a "power method" (see, e.g., [2], [22]). Since our proofs of Theorem 3.5 and 3.7 also use this method and since it is in the methodology, rather than in the corollaries of the analysis, that the discrete-time and the continuous-time cases are similar, we derive those methods in a form already appreciated in the 19th Century, but using the more modern matrix notation. Suppose A is a 2×2 real

matrix with entries a_{ij}, $i, j = 1, 2$, and consider the differential or difference equations

$$\frac{d}{dt}\begin{bmatrix} x \\ y \end{bmatrix} = A\begin{bmatrix} x \\ y \end{bmatrix} \quad (4.23a)$$

$$\begin{bmatrix} x \\ y \end{bmatrix}_{t+1} = A\begin{bmatrix} x \\ y \end{bmatrix}_t. \quad (4.23b)$$

Riccati noted that if the initial data $\begin{bmatrix} x_0 \\ y_0 \end{bmatrix}$ and $\begin{bmatrix} x_0' \\ y_0' \end{bmatrix}$ for (4.23a) were collinear, then the solutions $\begin{bmatrix} x_t \\ y_t \end{bmatrix}$ and $\begin{bmatrix} x_t' \\ y_t' \end{bmatrix}$ remain collinear for all t, i.e., that linear differential equations propagate lines as lines. Therefore, there must be a differential equation for the slope, $m_t = x_t / y_t$ which is computed as a "Riccati equation":

$$\dot{m}_t = a_{21} + (a_{22} - a_{11})m - a_{12}m^2.$$

And Riccati noted that any such equation could be solved as the ratio of the components y_t and x_t of a state evolving according to a linear differential equation. On the other hand, if A is invertible, then (4.23b) propagates lines to lines, so there must be a difference equation for the slope m_t. Indeed

$$m_{t+1} = \frac{a_{21} + a_{22}m_t}{a_{11} + a_{12}m_t}. \quad (4.24)$$

Conversely, any Möbius transformation corresponds to a matrix A and therefore Möbius iterations correspond to matrix iterations A^n, acting on lines. Moreover, A and A_1 define the same Möbius transformation over $\mathbb{R}$ or $(\mathbb{C})$ if and only if $A_1 = \mu A$ for some nonzero $\mu \in \mathbb{R}$ (or $\mu \in \mathbb{C}$). Note that while (4.24) is undefined for some m

$$l \mapsto Al \quad (4.25)$$

is always defined. In other words, the linear model (4.25) also contains the line with infinite slope, viz. $l = \text{span}\left\{ \begin{pmatrix} v_1 \\ v_2 \end{pmatrix} \right\}$ with $v_1 = 0$. This fact, coupled with linearity, makes this "state–costate" representation of a Möbius transformation as powerful as the state–costate representation of a Riccati equation. One can now quite easily prove Theorem 4.1, 1) and 2) by deriving a corresponding A, diagonalized either over $\mathbb{R}$ or $\mathbb{C}$ and then computing the iterates of a "conjugate" Möbius transform (although some care needs to be taken to see that (4.24) in the resulting division does not change the period or cause finite escape to infinity). As we shall see in Section V, Theorem 4.1, 3) and the more detailed discussion in Corollary 3.8 involve some rather important results from number theory. □

Remark 4.6: In Remark 4.5, we stressed the analogy between the analysis of continuous-time and discrete-time systems by state–costate methods. As Theorems 3.5, 3.7, and 4.1 show, however, it is here that the analogy stops. In Remark 3.11, we illustrated the well-known fact that for initial data where the positive real condition is volated, the solutions of the continuous-time Riccati equation always have finite escape time. In discrete-time, under the same conditions, some solutions (see Section V for an explicit parameterization) can escape in finite time. However, for parameters

not satisfying the positive real conditions, solutions can also

1) evolve in unbounded, complicated excursions; or
2) exhibit periodic behavior; or
3) converge to a classical limit.

Why, then, is the discrete-time case different from the continuous-time case? One possible answer would be the conventional wisdom that discrete-time m-dimensional systems behave more like continuous-time $(m + 1)$-dimensional systems. However, in continuous time, the finite escape behavior persists in higher dimensions. It is rather true for a different, but somewhat simple reason involving the analogous, but different, state–costate representations of continuous-time and discrete-time Riccati equations discussed in Remark 4.4. In discrete time, it is possible for the iterates $A^n l$ of a line l to jump over the "infinite" line, or vertical axis, say from right to left, without becoming infinite for some n, but for continuous time $e^{At} l$ cannot cross the infinite line without being infinite for some finite time, corresponding of course to finite escape time for the continuous-time Riccati equation. It is this difference that accounts for the rich dynamical behavior of discrete-time filtering algorithms, including the Riccati equation, for nonclassical initial data.   □

Let us conclude with another important point. We have expressed the Kalman filter in terms of the invariant Riccati equation (4.7), whereas it is more common to start from a specific stochastic system (4.4) and use the Riccati equation

$$p_{t+1} = a^2 p_t - \frac{(ap_t - bd')^2}{p_t + dd'} + bb' \qquad (4.26)$$

in terms of the state error covariance

$$p_t = E\{(x_t - \hat{x}_t)^2\}. \qquad (4.27)$$

At the price of somewhat more complicated formulas, we could have carried out our analysis in this framework instead, to obtain equivalent results to those of Theorem 4.1. Indeed, the Riccati equations (4.7) and (4.26) are related through

$$p_t = p_0 - \pi_t =: \psi(\pi_t) \qquad (4.28)$$

so that, if the dynamical systems (4.7) and (4.26) are denoted f and g, respectively, we have

$$\psi \bigcirc f = g \bigcirc \psi,$$

i.e., the dynamical systems are *topologically conjugate* [7]. In the state–costate formulation of Remark 4.5 this conjugacy is reflected in the fact that the corresponding A-matrices are similar modulo normalization.

Finally, we should stress that one of the reasons why we prefer to work with the fast filtering algorithm and to analyze the dynamics of the Riccati equation in terms of it is that all the parameters enter only in the initial conditions and not in the recursions themselves, thereby directly exhibiting the underlying invariance.

V. ANALYSIS OF DYNAMICS

In this section, we give proofs of Theorems 3.3, 3.5, 3.7, 4.1, and their corollaries.

Proof of Theorem 3.3:

1) If q_t^* and hence $Q_t^*(z)$, tends to zero as $t \to \infty$, then, by (2.28)

$$Q_\infty(z)Q_\infty(z^{-1}) = r_\infty D(z, z^{-1})$$

and therefore $D(z, z^{-1})$ is sign definite, and $Q_\infty(z)$ is a spectral factor as stated.

2) It was shown in [14] that if the initial data (q_0, q_0^*) satisfy the positive real condition, i.e., they correspond to an underlying stochastic system so that the usual conditions for Kalman filtering are satisfied, then q_t^* tends to zero as $t \to \infty$. Moreover, it is also shown in [16] that $Q_t(z)$ is stable for all $t = 0, 1, 2, \dots$, and that the same is true for $Q_\infty(z)$.

3) It remains to show that the sign indefinite region contains infinitely many periodic points of any period p, $p \geq 3$. To this end, note that if only the first components of q_0 and q_0^* are nonzero, the system (2.25) reduces to the system (3.10), and consequently the statement on this invariant submanifold follows from Theorem 3.7.   □

Recall that Theorem 3.5 is concerned with convergence of the fast algorithm (3.10) for initial data in the sign definite region of Fig. 2 (corresponding to hyperbolas (3.13) with $0 < \kappa^2 < 1$) and that Theorem 3.7 is concerned with periodic behavior and unbounded excursions for initial data in the "white corridors" of Fig. 2 (corresponding to hyperbolas (3.13) with $1 < \kappa^2 \leq \infty$). Let us first discard the case $\kappa^2 = \infty$. Here, the orbit lies on the hyperbola $\gamma^2 - \alpha^2 = 1$ on which the first of equations (3.10) takes the form

$$\alpha_{t+1} = -(\alpha_t)^{-1}$$

which is periodic with period 2. On the other hand, the second of equations (3.10) implies

$$\gamma_{t+2} = -\alpha_{t+2}\gamma_{t+1} = \alpha_{t+2}\alpha_{t+1}\gamma_t = -\gamma_t$$

so that each point (α_0, γ_0) is periodic with period 4.

Therefore, we can now limit our attention to κ such that $0 < \kappa^2 < \infty$. Using (3.13) to eliminate γ_t from the first of equations (3.10), the dynamical system (3.10) projects under the map $(\alpha, \gamma) \to \alpha$ to a dynamical system defined by a Möbius transformation

$$\alpha_{t+1} = \frac{\kappa}{2 - \kappa\alpha_t}. \qquad (5.1)$$

Invoking either the fundamental theorem of projective geometry or the power method, as reviewed in Section IV, we can compute iterates of (5.1) via iteration of a linear transformation unique up to a multiplicative constant, on the space of lines in $\mathbb{R}^2$. We chose the constant so that this transformation is symplectic, i.e., we consider the dynamical system

$$\begin{bmatrix} v_1 \\ v_2 \end{bmatrix}_{t+1} = \begin{bmatrix} 2/\kappa & -1 \\ 1 & 0 \end{bmatrix} \begin{bmatrix} v_1 \\ v_2 \end{bmatrix}_t \qquad (5.1')$$

where of course $\alpha_t = (v_2/v_1)_t$. The characteristic roots $\lambda_+(\kappa)$, $\lambda_-(\kappa)$ of the matrix

$$A(\kappa) = \begin{bmatrix} 2/\kappa & -1 \\ 1 & 0 \end{bmatrix}$$

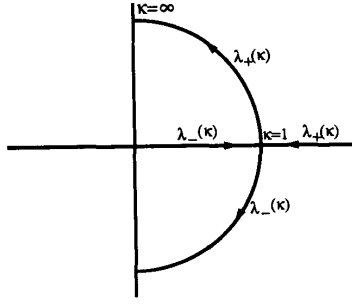obey the root-locus (or bifurcation) plot as depicted in Fig. 6.

Fig. 6.

For $0 < \kappa < 1$ there are two roots $\lambda_+(\kappa)$, $\lambda_-(\kappa)$ satisfying $\lambda_+(\kappa)\lambda_-(\kappa) = 1$ with $\lambda_+(\kappa) > \lambda_-(\kappa)$. The situation for $0 < -\kappa < 1$ is similar with $\lambda_-(\kappa)$ and $\lambda_+(\kappa)$ intercharged. For $|\kappa| > 1$ the roots $\lambda_\pm(\kappa)$ lie on the unit circle, in fact

$$\lambda_+(\kappa) = e^{\pm i\theta_\kappa} \tag{5.2a}$$

where

$$\theta_\kappa = \begin{cases} \arctan \sqrt{\kappa^2 - 1} & \text{if } \kappa > 1 \\ \pi - \arctan \sqrt{\kappa^2 - 1} & \text{if } \kappa < -1. \end{cases} \tag{5.2b}$$

We are now prepared to prove Theorems 3.5 and 3.7, as well as Theorem 4.1.

Proof of Theorem 3.5: Suppose $0 < \kappa < 1$, in which case $A(\kappa)$ has eigenvalues $\lambda_\pm(\kappa)$ with corresponding eigenvectors

$$v_+ = \begin{bmatrix} \lambda_+(\kappa) \\ 1 \end{bmatrix} \quad v_- = \begin{bmatrix} \lambda_-(\kappa) \\ 1 \end{bmatrix}.$$

It is easy to check that the slopes

$$\alpha_+(\kappa) = 1/\lambda_+(\kappa) = \lambda_-(\kappa) \quad \text{and}$$

$$\alpha_-(\kappa) = 1/\lambda_-(\kappa) = \lambda_+(\kappa)$$

of the lines $l_+ := \operatorname{span}\{v_+\}$ and $l_- := \operatorname{span}\{v_-\}$, respectively, are the equilibria of (5.1). We shall see that $\alpha_+(\kappa)$ is asymptotically stable and $\alpha_-(\kappa)$ is unstable.

For any $v \in \mathbb{R}^2$, there are real numbers β_+, β_- such that $v = \beta_+ v_+ + \beta_- v_-$, and so

$$A(\kappa)^t v = \beta_+ \lambda_+^t v_+ + \beta_- \lambda_-^t v_-.$$

Since

$$\operatorname{span}\{A(\kappa)^t v\} = \operatorname{span}\{\beta_+ v_+ + \beta_-(\lambda_-/\lambda_+)^t v_-\}$$

we see that the line $l_0 := \operatorname{span}\{v\}$ under iteration of $A(\kappa)$ converges to l_+, which, in terms of slopes, implies that $\alpha_t \to \alpha_+$. Moreover, in v_+, v_- coordinates the slope of $A(\kappa)^t l_0$ is

$$m_t = (\beta_-/\beta_+)(\lambda_-/\lambda_+)^t$$

so that $m_t \to 0$, as $t \to \infty$ monotonically. Therefore, the phase portrait of (5.1) is as in Fig. 7.

For any initial condition to the right of α_-, α_t increases monotonically until it jumps across infinity to the left of α_+,
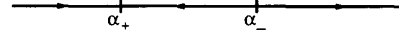

Fig. 7.

corresponding to a line l_o such that $A(\kappa)^{t+1} l_o$ jumps across the v_2 axis; then for $i \geq 1$, α_{t+i} tends monotonically increasing to α_+. Those initial data $\alpha^{(i)}$ which jump to infinity at step i are determined uniquely by the expression $\alpha^{(i)} = v_2^{(i)}/v_1^{(i)}$ where

$$\begin{bmatrix} v_1^{(i)} \\ v_2^{(i)} \end{bmatrix} = A^{-i} \begin{bmatrix} 0 \\ 1 \end{bmatrix}. \tag{5.3}$$

In particular, any $\alpha^{(i)}$ lies to the right of α_- and an analysis similar to the one given above in forward time shows that

$$\alpha^{(i)} \to \alpha_- \quad \text{as } i \to \infty$$

monotonically decreasing.

Finally, we note that points α_0 lying to the right of α_- correspond to a pair of points (α_0, γ_0), $(\alpha_0, -\gamma_0)$ lying on (3.13), and the evolution of (3.10) for such initial data on (3.13) is determined by analyzing (5.1). The same remark applies to those points lying to the left of α_+. Points lying between α_- and α_+ while initial data for monotonically convergent trajectories of (5.1) do not correspond to points (α_0, γ_0) on hyperbolas (3.13) with $0 < \kappa < 1$. (These points correspond to the second case in Corollary 4.3. Also see Remark 4.4.) The case $-1 < \kappa < 0$ follows, *mutatis mutandis*.

In view of (2.8), $d_t(z, z^{-1}) := r_t^{-1} D(z, z^{-1})$ and $d_{t+1}(z, z^{-1})$ have different signs if and only if $|\gamma_t| > 1$. Therefore a point in region III must jump to the negative region II in the next step and a point in region II to a positive region, which, by monotonicity, must be I. (Visiting region II corresponds to the only time at which (4.9) becomes negative when π_{t+1} just has jumped over ∞ temporarily becoming smaller than π_t). Also, a jump from IV to I in one step is impossible since this would imply that $|\gamma_t| < 1$ for all t which, by Schur's condition (2.9), is equivalent to positive realness, i.e., to the initial condition being in I. By the same condition, once it arrives in I, the sequence $\{(\alpha_t, \gamma_t)\}$ will stay there.

In the case $\kappa^2 = 1$, the hyperbola degenerates to a pair of boundary lines (between the sign definite and sign indefinite regions) through the unique equilibrium point $(1, 0)$ or $(-1, 0)$ depending on whether $\kappa = 1$ or $\kappa = -1$. The matrix $A(1)$ has an eigenvalue $\lambda = 1$ of (algebraic) multiplicity 2 but only one eigenvector $v_1 = \begin{bmatrix} 1 \\ 1 \end{bmatrix}$. Then any $v \in \mathbb{R}^2$ can be represented $v = \beta_1 v_1 + \beta_2 v_2$ where v_2 is the principal vector (generalized eigenvector) such that $(A - \lambda I)v_2 = v_1$, i.e., $A v_2 = v_1 + v_2$. Then

$$A^t v = (\beta_1 + \beta_2 t) v_1 + \beta_2 v_2$$

and consequently

$$l := \operatorname{span}\{A^t v\} = \operatorname{span}\left\{v_1 + \frac{\beta_2}{\beta_1 + \beta_2 t} v_2\right\} \to \operatorname{span}\{v_1\},$$

i.e., $\alpha_t \to 1$, monotonically as $t \to \infty$. In the same way, if $\kappa = -1$, $\alpha_t \to -1$ monotonically, when $t \to \infty$.   □

Proof of Theorem 4.1: Consider the Riccati equation (4.7) corresponding to an arbitrary pair (α_0, γ_0) of parameters. Let $\{\pi_t\}$ be the orbit of π_0. It is then straightforward to show that

$$\bar{\alpha}_t = \frac{\alpha_0}{1 - \pi_t} \qquad \text{for } t = 1, 2, 3, \cdots \qquad (5.4)$$

is the orbit of $\bar{\alpha}_0 = \alpha_0/(1 - \pi_0)$ under the dynamical system (5.1) where κ is defined by (4.13) in terms of (α_0, γ_0). In fact, the dynamical systems (4.7) and (5.1) are topologically conjugate. This is manifested by the relation

$$\begin{bmatrix} 1/\alpha_0^2 & -1/\alpha_0 \\ \gamma_0^2/\alpha_0 & (\alpha_0^2 - \gamma_0^2)/\alpha_0 \end{bmatrix}$$

$$= \begin{bmatrix} 1 & -1 \\ \alpha_0 & 0 \end{bmatrix}^{-1} \begin{bmatrix} 2/\kappa & -1 \\ 1 & 0 \end{bmatrix} \begin{bmatrix} 1 & -1 \\ \alpha_0 & 0 \end{bmatrix} \qquad (5.5)$$

which says that the linear map A for the Möbius transformation (4.7′), the left member, is similar to the linear map A of (5.1). Correspondingly, the dynamics of (4.7) is identical to that of (5.1) described above. For $|\kappa| < 1$ the equilibrium points p_+ and p_- correspond to α_+ and α_-, and now the interval between α_+ and α_- in Fig. 7 is part of the phase diagram. Initial points in this interval correspond to π_0 such that $\varphi(\pi_0) \le 0$, and such point cannot escape. Outside of this interval, corresponding to $\varphi(\pi_0) \ge 0$ there is finite escape for a set of points of measure zero.

If $1 < \kappa < \infty$, the eigenvalues $\lambda_\pm(\kappa)$ are complex with complex eigenvectors $v_\pm(\kappa)$. If v is a real nonzero vector then v can be expressed as

$$v = \beta_+(\kappa)v_+(\kappa) + \beta_-(\kappa)v_-(\kappa)$$

where $\overline{\beta_+(\kappa)} = \beta_-(\kappa)$. As before

$$A(\kappa)^t v = \beta_+(\kappa)\lambda_+^t(\kappa)v_+(\kappa) + \beta_-(\kappa)\lambda_-^t(\kappa)v_-(\kappa)$$

$$= \beta_+(\kappa)e^{it\theta}v_+(\kappa) + \beta_-(\kappa)e^{-it\theta_\kappa}v_-(\kappa).$$

Since $A(\kappa)^t v$ is real, the motion of the first component determines the evolution of $l_0 := \text{span}\{v\}$ in $\mathbb{R}^2$.

According to Kronecker (see [13]), the subset

$$S_{\theta_\kappa} = \{e^{it\theta_\kappa} : t \in \mathbb{Z}\} \subset S^1$$

is either finite, if θ_κ is rationally dependent on π, or dense if θ_κ is rationally independent from π. We are, of course, taking a forward orbit, so that only terms such as $e^{it\theta_\kappa}$, $t = 0, 1, 2, \cdots$ occur in the $v_+(\kappa)$ coefficient of $A(\kappa)^t v$. On the other hand, l_0 intersects the unit circle in $e^{i\theta_v}$ (and also in the antipodal point $e^{i(\theta_v + \pi)}$) so that $A(\kappa)^t l_0$ intersects the unit circle S^1 in

$$S_{\theta_\kappa} \cdot e^{i\theta_v} = \{e^{it\theta_\kappa + i\theta_v} : t \in \mathbb{Z}\}.$$

In particular, the orbit of the slope α_t of $A(\kappa)^t l_0$ is either periodic or dense, according as to whether θ_κ as defined in (5.3) is a rational multiple of π or not. Furthermore, if

$\theta_\kappa = (n/d)\pi$, then recalling that $e^{i\theta}$ and $e^{i(\theta + \pi)}$ are antipodal points lying on the same line, we see that

$$A(\kappa)^p l = l$$

for all l, and d is the smallest natural number with this property provided $(n, d) = 1$, i.e., n and d are coprime. Moreover, any $d \ge 2$ can occur.

We note that when $|\kappa| > 1$, we always have $\varphi(\pi_0) \ge 0$ and cases 2) and 3) occur except for the measure zero set of finite escape points, which we now describe. In the case $\arctan \sqrt{\kappa^2 - 1} \notin \mathbb{Q}\pi$, the point which escapes at time i is defined by $\alpha^{(i)} = v_1^{(i)}$ where

$$\begin{bmatrix} v_1^{(i)} \\ v_2^{(i)} \end{bmatrix} = A^{-i} \begin{bmatrix} 0 \\ 1 \end{bmatrix}, \qquad i = 1, 2 \cdots. \qquad (5.6)$$

In particular, such points form a dense countable subset of the hyperbola. In case $\arctan \sqrt{\kappa^2 - 1} = n\pi/d$, where $(n, d) = 1$, then a point escapes at time i if and only if $i = 1, \cdots, d - 1$.   □

Proof of Theorem 3.7: We remark that in the case $\kappa^2 > 1$, the hyperbola (3.13) is a 2-1 "covering" of the α-axis, the trajectory α_t of (5.1) initialized at α_0 corresponding to two trajectories $(\alpha_t, \pm \gamma_t)$ of (3.10) initialized at $(\alpha_0, \pm \gamma_0)$ in accordance with Theorem 3.2. Thus, it conceivably could occur that on the hyperbola containing $(\alpha_0, \pm \gamma_0)$ the pair of trajectories $(\alpha_t, \pm \gamma_t)$ is dense while neither trajectory is dense. However, this does not happen, as we see by the change of coordinates

$$a = \alpha - \gamma, \qquad b = \alpha + \gamma.$$

In the new coordinates, the hyperbola takes the form depicted in Fig. 8 while a_t itself evolves according to the Möbius iteration

$$a_{t+1} = \frac{a_t - 1}{a_t - 2\lambda + 1} \qquad (5.7)$$

where $\lambda = 1/\kappa$. As before, this Möbius transformation corresponds to a linear transformation A_1 with matrix representation

$$A_1 = \begin{bmatrix} 1 - 2\lambda & 1 \\ -1 & 1 \end{bmatrix} \qquad (5.8)$$

and characteristic polynomial

$$s^2 - 2s + 2 + \lambda(2s - 2)$$

yielding the root-locus plot, as shown in Fig. 9, the right-half corresponding to positive λ and the left to negative λ. In particular, (5.5) has complex eigenvalues if and only if $|\lambda| < 1$, i.e., if and only if $|\kappa| > 1$. Therefore, for $|\kappa| > 1$, the system (5.7) has either all periodic points or all dense trajectories. Moreover, since each point on such a hyperbola is in one-one correspondence to a point on the a-axis, to say all trajectories of (5.7) are dense on the real line is to say that all trajectories of (α_t, γ_t) are dense on the hyperbola containing the initial data, which is what we wished to prove.

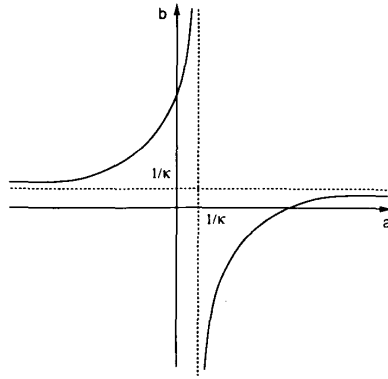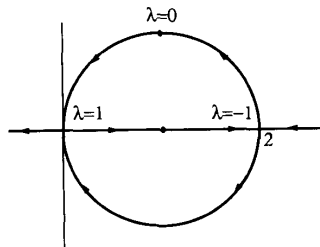Another consequence of the 2-1 correspondence with the
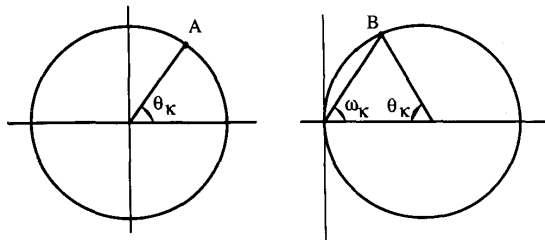
Fig. 8.

Fig. 9.

Fig. 10.

hyperbola to the α-axis is that, while α_t might be periodic with period d, (α_t, γ_t) could have period d or $2d$. Since a_t has the same period as (α_t, γ_t), it therefore remains to investigate the relationship between the periods of a_t and α_t. To this end, first note that

$$A_1 = I - A,$$

i.e., the root locus of (5.7) is obtained from that of (5.1) by mirroring in the imaginary axis and then translating one step to the right.

Fig. 10 depicts the parts of the root loci for which $|\kappa| > 1$, and points A and B have the same κ. Elementary geometry shows that the corresponding angles θ_κ and ω_κ are related through the equation

$$\omega_\kappa = (\pi - \theta_\kappa)/2$$

where θ_κ is given by (5.2b). Now, if the period of (α_t, γ_t), and hence of a_t, is p, i.e., $\omega_\kappa = (q/p)\pi$ with $(q, p) = 1$,

then

$$\theta_\kappa = \frac{p - 2q}{p}\pi$$

and $(p - 2q, p)$ equals either 1 if p is odd, or 2 if p is even. Consequently, the period d of α_t is p if p is odd, and $p/2$ if p is even. From Fig. 10, we see that ω_κ can take any value on the interval $(0, \pi/2)$, and therefore all periods $p \geq 3$ are possible. However, it is not hard to see that, for example, $p = 3$ can be achieved only for a positive κ and $p = 6$ only for a negative κ. Recalling that when $\kappa^2 > 1$, the hyperbola (3.13) is a 2–1 covering of the α-axis, the $d - 1$ points defined by (5.6) correspond to $2(d - 1)$ points lying on the hyperbola and escaping to infinity, two each at times $t = 1, \cdots, d - 1$. Since $d = p$ when p is odd and $p = 2k$ when p is even, the corresponding statement of the theorem follows. $\square$

Proof of Corollary 3.8: In general, the possible periods which can be realized by a trajectory initialized on (3.13) with $\kappa > 1$ correspond to those natural numbers p for which there exists a relatively prime natural number q, $1 \leq q < p$, satisfying

$$\frac{1}{4} \leq \frac{q}{p}\pi < \frac{1}{2}\pi. \tag{5.9}$$

For $\kappa < -1$ the possible periods p are characterized by the existence of such a natural number satisfying in lieu of (5.9)

$$0 \leq \frac{q}{p}\pi \leq \frac{1}{4}\pi. \tag{5.10}$$

It is clear that the second inequality is satisfied, by taking $q = 1$ for all $p \geq 4$. Conversely, for $p = 1, 2, 3$ no such q exists. Our analysis of the case $\kappa > 1$ reposes on the following number-theoretic lemma.

Lemma 5.1: For every integer p, $p \geq 3$, and $p \neq 6$, there exists an integer q, $1 \leq q < p$ such that (5.6) holds and $(p, q) = 1$. Moreover, no such integer exists if $p = 1$, 2, or 6.

Proof: That no such integer exists for $p = 1, 2,$ or 6 is obvious. For $3 \leq p \leq 5$ and $7 \leq p \leq 9$ the assertion is clear. For $p \geq 10$, consider the inequality

$$[p/4] < q < 2[p/4] \tag{5.11}$$

where for a rational number x, $[x]$ denotes the greatest integer less than or equal to x. Setting $p = 4r + s$, $0 \leq s \leq 3$, we see that if q satisfies (5.11), then q satisfies (5.9). According to Bertrand's postulate [13], there exists a prime number p' for which $q = p'$ satisfies (5.11). First, suppose $p = 4r$. Since $p' > r \geq 2$, p' cannot be a prime factor of p, so that setting $q = p'$ yields $(p, q) = 1$. Similarly, if $p = 4r + 2$, then to say p' divides p is to say p' divides $2r + 1$ which is impossible since $p' \geq r + 1$. Therefore, if $q = p'$, then $(p, q) = 1$. Next, consider the case $p = 4r + 1$. If p' divides p, we must have $p = dp'$ with $d = 2$ or $d = 3$. Since p is odd, we must have $p = 3p'$. It is also clear that $p' + 1$ must satisfy (5.11), and, since $p > 9$, and hence $r > 2$, $p' - 1 > r$. Therefore, both $p' + 1$ and $p' -$

1 satisfy (5.11). Since not both $p' + 1$ and $p' - 1$ are divisible by 3 and neither are divisible by p', $(p, q) = 1$ for at least one choice, $q = p' \pm 1$. Finally, suppose $p = 4r + 3$. Then, as above, to say $(p, p') \neq 1$ is to say $p = 3p'$ is a prime factorization. Again $p' + 1$ satisfies (5.11) and $p' - 1 = r$ only if $r = 0$ and therefore $p = 3$. Since $p \geq 10$, we see from (5.11) that at least in our case, $q = p' \pm 1$, satisfies the conditions of the lemma. $\qquad \square$

Proof of Corollary 4.2: If $\varphi(\pi_0) \geq 0$, there is a sequence $\{\gamma_t\}$, so far defined only upto sign, so that (4.19) holds. Then inserting (4.16), which is obtained from (5.7), into (4.19) we obtain the first of equations (4.14), where, for simplicity, we drop the bar over α. Now eliminating α_{t+1} between this equation and (5.1) yields the integral curve (4.15). Finally, inserting $2\alpha_{t+1}/\kappa = 1 + \alpha_{t+1}\alpha_t$, obtained from (5.1), into (4.15) at $t + 1$ yields

$$\gamma_{t+1}^2 = \alpha_{t+1}^2 \left(1 - \frac{\alpha_t}{\alpha_{t+1}} \right) = \alpha_{t+1}^2 \gamma_t^2$$

where, in the last equality, the first of equations (4.14) has been used. Then fixing the sign of $\{\gamma_t\}$ so that $\gamma_{t+1} = -\alpha_{t+1}\gamma_t$, the second of equations (4.14) is established. The analysis for the case $\varphi(\pi_0) \leq 0$ is analogous only exchanging γ_t for $i\gamma_t$. Clearly, $\varphi(p)$ will take negative values if and only if there are real roots, which occurs precisely when $|\kappa| \leq 1$. $\qquad \square$

V. CONCLUSION

In this paper, we initiated an analysis of the discrete-time Kalman filter as a nonlinear dynamical system, stressing the existence of both highly regular and unpredictable dynamical behavior. Our analysis is motivated by a desire to understand the asymptotic dependence of the Kalman filter on the parameters determining it, since in many situations of interest, these parameters have to be estimated. For example, even in Kalman filtering of systems in statistical steady state, the filtering equations often rely on estimates of either covariance data or noise intensities. And since such estimates may or may not correspond to statistics generated by an underlying stochastic system, it is important to understand the convergence properties and the sensitivity to variation in parameters of the Kalman filter, for arbitrary parameters. As is well known, parameters corresponding to a stochastic system satisfy various positivity constraints reflecting either positive definiteness of the infinite covariance matrix or positive realness of the corresponding modeling filter. On the other hand, it has been known for some time that such positivity conditions are not necessary for convergence of the Kalman filter. In this paper, we identified a general necessary condition for convergence of the Kalman filter with given initial data. In the case of a one-dimensional system, this is also sufficient but we have shown that, much more surprisingly, in the complement of this region of attraction, the Kalman filter is extremely sensitive to initial data. Indeed, there exists an uncountably infinite dense set of periodic points of each period p, $p \geq 2$, or 3 (depending on the algorithm), an uncountable dense set of points having unbounded trajectories and an uncountable dense set of initial data having finite

escape time. In the one-dimensional case we are able, using an analysis of Möbius transforms via "power methods," to give a complete phase portrait which is seemingly in sharp contrast to phase portraits of the continuous-time Riccati equation [20], [25], [27], suggesting that the discrete-time case, in any dimension, is far more complicated than the continuous-time case, even after the typical dimension reduction. In fact, using an imbedding technique we show that these and several other dynamical properties persist for Kalman filtering in arbitrary dimensions.

REFERENCES

[1] N. I. Akhiezer, *The Classical Moment Problem.* New York: Hafner, 1965.
[2] G. Ammar and C. Martin, "The geometry of matrix equivalence methods," *Acta Appliance Mathematicae,* vol. 5, pp. 239–278, 1986.
[3] E. Artin, *Geometric Algebra.* New York: Interscience, 1957.
[4] C. I. Byrnes and A. Lindquist, "On the geometry of the Kimura–Georgiou parametrization of modelling filters," *Int. J. Contr.,* vol. 50, pp. 2301–2312, 1989.
[5] C. I. Byrnes, A. Lindquist, and Y. Zhou, *Stable, Unstable and Center Manifolds for Fast Filtering Algorithms,* to be published.
[6] P. E. Caines, *Linear Stochastic Systems.* New York: Wiley, 1988.
[7] R. L. Devaney, *An Introduction to Chaotic Dynamic System.* Reading, MA: Addison-Wesley, 1987.
[8] P. Faurre, M. Clerget, and F. Germain, *Operateurs Rationels Positifs.* Paris, France: Dunod, 1979.
[9] T. T. Georgiou and P. P. Khargonekar, "Linear fractional transformations and spectral factorization," *IEEE Trans. Automat. Contr.,* vol. AC-31, pp. 345–347, 1986.
[10] L. Ya. Geronimus, *Orthogonal Polynomials.* Consultant Bureau, New York, 1961.
[11] M. R. Gevers, R. R. Bitmead, I. R. Petersen, and R. J. Kaye, "When is the Riccati equation stabilizing at every instant?" in *Frequency Domain and State Space Methods for Linear Systems,* C. I. Byrnes and A. Lindquist, Eds. Amsterdam, The Netherlands, North Holland, 1986, pp. 531–540.
[12] U. Grenander and G. Szegö, *Toeplitz Forms and Their Applications.* Berkeley, CA: Univ. California Press, 1958.
[13] G. H. Hardy and E. M. Wright, *An Introduction to the Theory of Numbers.* Oxford: Clarendon, 1954.
[14] N. Levinsson, "The Wiener rms (root mean square) error in filter design and prediction," in *Extrapolation, Interpolation and Smoothing of Stationary Time Series,* Wiener. Cambridge, MA: M.I.T. Press, 1942, Appendix 13.
[15] A. Lindquist, "A new algorithm for optimal filtering of discrete-time stationary process," *SIAM J. Contr.,* vol. 12, pp. 736–746.
[16] ——, "Some reduced-order non-Riccati equations for linear least-squares estimation: The stationary, single-output case," *Int. J. Contr.,* vol. 24, pp. 821–842, 1976.
[17] ——, "Linear least-square prediction based on convariance data from stationary processes with finite-dimensional realizations," in *Proc. Second European Congress on Operations Research,* Stockholm, Sweden, 1976, pp. 281–285.
[18] A. Lindquist and G. Picci, "On the stochastic realization problem," *SIAM J. Contr. Optimiz.,* vol. 17, pp. 365–389, 1979.
[19] ——, "Realization theory for multivariate stationary Gaussian processes," *SIAM J. Contr. Optimiz.,* vol. 23, pp. 809–857, 1985.
[20] C. F. Martin, "Grassmanian manifolds, Riccati equations and feedback invariants of linear systems," *Geometrical Methods for the Theory of Linear Systems,* C. I. Byrnes and C. F. Martin, Eds. Dordrecht, The Netherlands: Reidel, 1980, pp. 195–211.

[21] C. Martin, "Finite escape time for Riccati differential equations," *Syst. Contr. Lett.*, vol. 1, pp. 127-131.

[22] B. N. Partlett and W. G. Poole, "A geometric theory for the QR, LU and power iterations," *SIAM J. Numer. Anal.*, vol. 10, pp. 389-412, 1973.

[23] M. Pavon, "Stochastic realization and invariant directions of the matrix Riccati equation," *SIAM J. Contr. Optimiz.*, vol. 18, pp. 155-180, 1980.

[24] I. Schur, "On power series which are bounded in the interior of the unit circle I and II," in *J. Für die reine und angewandte Mathematik*, vol. 148, pp. 122-145, 1918.

[25] M. A. Shayman, "Phase protrait of the matrix Riccati equation," *SIAM J. Contr. Optimiz.*, vol. 24, pp. 1-65, 1986.

[26] D. R. Vaughan, "A nonrecursive algebraic solution for the discrete Riccati equation," *IEEE Trans. Automat. Contr.*, vol. AC-15, pp. 597-599, 1970.

[27] J. C. Willems, "Least squares stationary optimal control and the algebraic Riccati equation," *IEEE Trans. Automat. Contr.*, vol. AC-16, pp. 621-634, 1971.

Christopher I. Byrnes (M'80-SM'85-F'89) was born in New York, NY, on June 28, 1949. He received the B.S. degree from Manhattan College, Bronx, NY, in 1971 and the M.S. and Ph.D. degrees from the University of Massachusetts, Amherst, in 1973 and 1975, respectively.

He served as an Instructor in the Department of Mathematics at the University of Utah, Salt Lake City, from 1975 to 1978, when he was appointed to Assistant Professor in the Department of Mathematics and in the Division of Applied Sciences at Harvard University, Cambridge, MA. From 1982 to 1985, he was Associate Professor of Applied Mathematics on the Gordon McKay Endowment at Harvard University. In 1984, he joined Arizona State University, Tempe, as a Research Professor of Engineering and Mathematics and also served as Adjunct Professor of Mathematical System Theory at the Royal Institute of Technology (KTH), Stockholm, Sweden from 1986 to 1990. He is currently Chairman and Professor in the Department of Systems Science and Mathematics at Washington University, St. Louis, MO. He has also held visiting positions at Bremen, Groningen, Harvard, IIASA, Kansas, KTH, Osaka, Paris-Dauphine, Rome-La Sapienza, Stanford, Tokyo, and with the Academy of Sciences of the USSR. His research interests include adaptive control, algebraic system theory, distributed parameter systems, linear multivariable control, and, most recently, in nonlinear control and the applications of nonlinear dynamics in control and estimation.

Dr. Byrnes is an editor of eleven research volumes and author of over 100 technical articles. He has served as an Associate Editor of four journals and is currently Editor of the two book series, *Systems and Control: Foundations and Applications* and *Progress in Systems and Control* (Boston: Birkhauser).
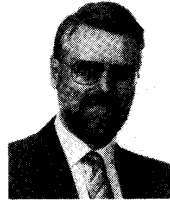
Anders Lindquist (M'77-SM'86-F'89) was born in Lund, Sweden, in 1942, He received the Ph.D. degree from the Royal Institute of Technology, Stockholm, Sweden, and in 1972 he was appointed a Docent there.

From 1972 to 1974, he held visiting positions at the University of Florida, Brown University, and University of Kentucky. In 1974, he became Associate Professor, and in 1980, Professor of Mathematics at the University of Kentucky, Lexington, KY, where he remained until 1983. He is presently a Professor at the Royal Institute of Technology, Stockholm, Sweden, where in 1982, he was appointed to the Chair of Optimization and Systems Theory, and an Affiliate Professor at Washington University, St. Louis, MO. He has also held visiting positions at University of Padova, Italy, University of Arizona, USSR Academy of Sciences, Moscow, and East China Normal University, Shanghai. From 1975 to 1976, he was a SIAM Visiting Lecturer.

Dr. Lindquist is the author of many papers in the area of systems and control, especially stochastic control, filtering, stochastic systems theory, realization theory, and applications of nonlinear dynamics in estimation and control, and he is an Editor of four research volumes. He is a Regional Editor of the *Journal of Mathematical Systems, Estimation, and Control* and an Associate Editor of *Systems and Control Letters*. He also serves on the editorial boards of *Adaptive Control and Signal Processing* and of the two book series, *Systems and Control: Foundations and Applications* and *Progress in Systems and Control* (Boston, MA: Birkhäuser).

Tone Lisbet Carlsen McGregor was born in Oslo, Norway, in 1962. She received the Bachelor of Computer Engineering and the B.S. in computer science in 1986 from the University of Minnesota, Duluth. After graduating, Tone returned to Scandinavia and worked developing robotics for Norsk Kybernettikk in Oslo, Norway. She returned to academia in 1987 by enrolling in the M.S.E.E. program at Arizona State University (ASU), Tempe, AR. She received the M.S.E.E. in control theory from ASU in 1989.

Currently, she is employed by Honeywell Inc. Commercial Flight Systems Group, Phoenix, AZ. Her responsibilities include system design and verification of flight guidance controls for the Canadair CL 601 and British Aerospace 1000.